*J. Fluid Mech.* (2017), *vol.* 827, *pp.* 31–66.  
doi:10.1017/jfm.2017.485

# Consistent formulations for stability of fluid flow through deformable channels and tubes

**Ramkarn Patne[1], D. Giribabu[1] and V. Shankar[1,†]**

[1]Department of Chemical Engineering, Indian Institute of Technology, Kanpur, 208016, India

(Received 14 March 2017; revised 31 May 2017; accepted 11 July 2017)

In the formulation of stability of fluid flow through channels and tubes with deformable walls, while the fluid is naturally treated in an Eulerian framework, the solid can be treated either in a Lagrangian or Eulerian framework. A consistent formulation, then, should yield results that are independent of the chosen framework. Previous studies have demonstrated this consistency for the stability of plane Couette flow past a deformable solid layer modelled as a neo-Hookean solid, in the creeping-flow limit. However, a similar exercise carried out in the creeping-flow limit for the stability of pressure-driven flow in a neo-Hookean tube shows that while the flow is stable in the Lagrangian formulation, it is unstable in the existing Eulerian formulation. The present work resolves this discrepancy by presenting consistent Lagrangian and Eulerian frameworks for performing stability analyses in flow through deformable tubes and channels. The resolution is achieved by making important modifications to the Lagrangian formulation to make it fundamentally consistent, as well as by proposing a proper formulation for the neo-Hookean constitutive relation in the Eulerian framework. In the neo-Hookean model, the Cauchy stress tensor in the solid is proportional to the Finger tensor. We demonstrate that the neo-Hookean constitutive model within the Eulerian formulation used in the previous studies is a special case of the Mooney–Rivlin solid, with the Cauchy stress tensor being proportional to the inverse of the Finger tensor unlike in a true neo-Hookean solid. Remarkably, for plane Couette flow subjected to two-dimensional perturbations, there is perfect agreement between the results obtained using earlier Eulerian and Lagrangian formulations despite the crucial difference in the constitutive relation owing to the rather simple kinematics of the base state. However, the consequences are drastic for pressure-driven flow in a tube even for axisymmetric disturbances. We propose a consistent neo-Hookean constitutive relation in the Eulerian framework, which yields results that are in perfect agreement with the results from the Lagrangian formulation for both plane Couette and tube flows at arbitrary Reynolds number. The present study thus provides an unambiguous formulation for carrying out stability analyses in flow through deformable channels and tubes. We further show that unlike plane Couette flow and Hagen–Poiseuille flow in rigid-walled conduits where there is a remarkable similarity in the linear stability characteristics between these two flows, the stability behaviour for these two flows is very different when the walls are deformable. The instability of plane Couette flow past a deformable wall is very robust and is not sensitive to the constitutive nature of the solid, but the stability of

† Email address for correspondence: vshankar@iitk.ac.in

pressure-driven flow in a deformable tube is rather sensitive to the constitutive nature of the deformable solid, especially at low Reynolds number.

**Key words:** biological fluid dynamics, flow–vessel interactions, instability

## 1. Introduction

In contrast to laminar–turbulent transition in rigid tubes and channels, it has been recently experimentally well-established (Kumaran & Muralikrishnan 2000; Eggert & Kumar 2004; Verma & Kumaran 2012, 2013; Kumaran 2015; Neelamegam & Shankar 2015; Srinivas & Kumaran 2015, 2017) that instability and transition in tubes and channels with deformable walls can occur at Reynolds numbers (∼200–800) much lower than their rigid counterparts, and that the transition is significantly affected by the elastic modulus of the deformable wall. There have been several efforts on the theoretical side over the last two decades which revealed qualitatively different mechanisms of the instability that arises when the dynamics of the perturbations in the fluid and solid are coupled (Shankar 2015). Despite the substantial progress made in this subject, several fundamental issues in the formulation of the problem remain unresolved.

Earlier theoretical studies (e.g. Kumaran 1995*b*, 1998; Shankar & Kumaran 1999, 2000) used the linear elastic solid model for modelling the deformations in the solid, which is strictly valid only in the limit of infinitesimal strains (Malvern 1969). However, even in a linear stability analysis involving only infinitesimal perturbations (and hence infinitesimal perturbation strains in the solid), the base state strain in a soft, deformable solid is not necessarily small under experimental conditions. Hence, as first pointed out by Gkanis & Kumar (2003), consistency demands that a frame-invariant model valid at finite deformations, such as the neo-Hookean model, must be used to model deformations in the solid. Gkanis & Kumar (2003) showed that for planar Couette flow, in the creeping-flow limit, results from both the linear elastic and neo-Hookean models agree qualitatively when the ratio of solid to fluid thickness is greater than unity. A similar exercise carried out for Hagen–Poiseuille flow in a deformable tube in the creeping-flow limit, however, found that the linear elastic model predicted an instability (Kumaran 1995*b*) but the neo-Hookean formulation did not (Gaurav & Shankar 2009). This discrepancy points to the need for a fundamentally consistent formulation that unambiguously predicts the presence or absence of an instability.

A first step in this direction was taken by Chokshi & Kumaran (2008*a*) for plane Couette flow past a deformable (neo-Hookean) solid layer, where they demonstrated that both Eulerian and Lagrangian formulations for the solid yield the same result consistent with that of Gkanis & Kumar (2003). It must be noted that while the fluid is naturally treated in an Eulerian framework, the deformable solid could be treated either in a Lagrangian or an Eulerian framework. However, as we explain in detail later in this paper, our attempts at an extension of the approach of Chokshi & Kumaran (2008*a*) failed to resolve the above-mentioned discrepancy for the stability of Hagen–Poiseuille flow in a deformable neo-Hookean tube, with their Eulerian and Lagrangian formulations yielding drastically different results. With the advent of many experimental studies carried out to validate theoretical predictions, there is a genuine need for an unambiguous formulation for the stability of the coupled

fluid–solid problem, which is consistent for different geometric configurations. With this motivation, in the present study, we develop consistent Lagrangian and Eulerian formulations for the coupled fluid–solid problem and demonstrate this for plane Couette flow and, importantly, for Hagen–Poiseuille flow in a deformable tube. We thereby arrive at a resolution to the puzzle regarding the question of stability of Hagen–Poiseuille flow in a neo-Hookean tube. In the remainder of this introduction, we briefly review the relevant previous theoretical efforts and place the present work in the context of the existing literature.

The study of the stability of fluid flow past deformable surfaces has its origins in the understanding of the phenomenon of drag reduction due to transition delay by the compliant surface, and most of the earlier studies had focussed on external (i.e. boundary layer) flows past a compliant surface (Benjamin 1960; Landahl 1962; Benjamin 1963; Carpenter & Garrad 1985, 1986; Carpenter & Gajjar 1990; Carpenter & Morris 1990). In contrast, 'internal' flows in conduits and tubes with deformable walls are also very relevant to many biological flows (Grotberg & Jensen 2004; Grotberg 2011), as well as to microfluidic flows in tubes and channels made of soft elastomers (McDonald & Whitesides 2002; Squires & Quake 2005), especially in the context of a manyfold increase of mass transfer rates in the unstable flow regime (Shrivastava, Cussler, & Kumar 2008; Kumaran & Bandaru 2016). While there have been some early attempts at the stability of internal flows in conduits with deformable walls (Garg 1977; Krindel & Silberberg 1979; Davies & Carpenter 1997), a systematic study of internal flows in deformable tubes and channels was initiated by Kumaran and co-workers (e.g. Kumaran 2003), wherein the linear elastic solid model was used to describe the deformations in the solid. These studies have established that there are two qualitatively different unstable modes in the high Reynolds number regime: (i) 'inviscid modes' in which the critical Reynolds number for instability is proportional to $G^{1/2}$ and (ii) 'wall modes' in which the critical Reynolds number is proportional to $G^{3/4}$, where $G$ is the shear modulus of the deformable wall. While the presence of inviscid modes is somewhat specific to the geometry and/or the nature of disturbances (axisymmetric versus non-axisymmetric), wall modes are a generic class of unstable modes that are present in any viscous shear flow past a deformable solid surface.

An important ingredient in the theoretical analysis to solve the coupled fluid–solid problem is the model used to describe the constitutive nature of the deformable solid. While earlier studies (see Kumaran 1995*a*,*b*; Shankar & Kumaran 1999, for example) had used the linear elastic model for the solid, later work by Gkanis & Kumar (2003, 2005), Chokshi & Kumaran (2008*a*,*b*) has demonstrated the importance of using a nonlinear elastic description more appropriate for finite deformations in the base state. In the base state, there is a balance between viscous stresses in the fluid ($\sim V\eta/R$) and elastic stresses in the solid ($\sim G$), and this balance yields $\Gamma \equiv V\eta/GR$, where $\Gamma$ is a non-dimensional quantity and is the ratio of viscous stresses in the fluid to elastic stresses in the solid, which is also a measure of the strain in the base state of the solid. Here, $V$, $\eta$, $G$ and $R$ are respectively the velocity scale in the base flow, viscosity of the fluid, shear modulus of the solid and length scale of the flow geometry.

In the high Reynolds number ($Re$) regime, previous studies (using the linear elastic model) have shown that the critical value of $\Gamma \propto Re^{-1/3}$ for wall modes (Shankar & Kumaran 2001, 2002), while for inviscid modes, $\Gamma \propto Re^{-1}$ (Shankar & Kumaran 1999, 2000). Thus, in the $Re \gg 1$ regime, the critical value of base state strain $\Gamma$ required for instability is asymptotically small, thereby rendering the predictions obtained using the linear elastic model internally consistent. Hence it can be expected

that the linear elastic solid would yield qualitatively correct results in the $Re \gg 1$ limit. Indeed, subsequent studies of Gaurav & Shankar (2009, 2010) using the neo-Hookean model have shown that the stability results are rather insensitive to the nature of the constitutive relation used to model the solid deformation at high $Re$. Experimental results (Verma & Kumaran 2012, 2013), however, indicate instability in tubes and channels with deformable walls occur at $Re \sim 200$–$800$, and it is not *a priori* clear whether theoretical predictions using the linear elastic model would be valid at this moderate Reynolds number.

In the limit of very low Reynolds number, theoretical predictions using the linear elastic solid model show that there is an instability when the parameter $\Gamma$ exceeds a critical value for all the canonical unidirectional shear flows (*viz.*, plane Couette flow, plane Poiseuille flow and Hagen–Poiseuille flow). The most unstable mode corresponds to wavelengths comparable to the tube radius or channel width, and hence this instability referred to as a 'finite-wave' instability. However, in the $Re \ll 1$ regime, the critical value of the parameter $\Gamma$ is typically $O(1)$ when the flow is unstable, thus raising a question on the applicability of the linear elastic model for describing deformations in the solid. This was first addressed by Gkanis & Kumar (2003) for plane Couette flow of a Newtonian fluid in the creeping-flow limit where the solid was modelled using the (frame-invariant) neo-Hookean model valid at finite strains in the solid. They showed that the use of neo-Hookean model introduces a new instability at high wavenumber (or, short wavelength, i.e. at wavelengths much smaller than the channel width) driven by the first normal stress difference in the base state, which is absent in the linear elastic model (Kumaran, Fredrickson & Pincus 1994). This new instability leads to differences in the predictions of critical value of $\Gamma$ required for instability for $H < 1$, but both models predict similar results for $H > 1$, where $H$ is the ratio of thickness of solid to fluid (Gkanis & Kumar 2003). This characteristic presence of high-wavenumber instability arising in the neo-Hookean model has also been confirmed for plane Poiseuille flow (Gkanis & Kumar 2005), but due to the use of inconsistent interface conditions, Gkanis & Kumar (2005) also predicted the presence of finite-wave instability in the creeping-flow limit, which was later shown to be absent by Gaurav & Shankar (2010) by using consistent interface conditions.

The Lagrangian formulation (for the solid) of Gkanis & Kumar (2003, 2005) uses the position coordinates of material points in the unstressed state as the independent variables. Henceforth, this Lagrangian formulation will be referred as the 'L2' formulation for the sake of brevity. The notation L2 refers to the Lagrangian formulation having two states, *viz.*, undeformed and perturbed states, as the relevant states of description in the solid. As discussed by Gaurav & Shankar (2010), in the L2 formulation, it is necessary to Taylor expand the base state fluid quantities from pre-stressed state to the undeformed state. This step is ambiguous as base state deformations in the solid are finite and hence the Taylor series expansion cannot be truncated to the linear order. One of the effects of the above inconsistency was the need to multiply fluid quantities with an exponential pre-factor (which arises while deriving interfacial conditions) that multiplies all the (homogeneous) interface conditions in the eigenvalue problem, thus leaving the eigenvalue unaffected. In the present work, we show that the use of the modified L3 formulation proposed in the paper removes the above inconsistencies in the formulation of the linearized conditions at the interface. In the ensuing discussion, the L2 formulation as proposed in the work of Gaurav & Shankar (2010) will be referred as 'old L2' formulation, and the proposed consistent L2 formulation as simply the 'L2' formulation. The

old L2 formulation and the L2 formulation proposed in this work differ only in the treatment of the linearized interface conditions.

Gaurav & Shankar (2009) further predicted that there is no finite-wave instability in the creeping-flow limit for flow in a deformable tube modelled using the neo-Hookean model, which contradicts the earlier predictions of Kumaran (1995*b*). Verma & Kumaran (2012, 2013) experimentally studied the plane Poiseuille and Hagen–Poiseuille flow with deformable walls, and observed that the theoretical predictions (using the neo-Hookean model) and experimental observations for the transition Reynolds number do not agree. Similarly, Neelamegam & Shankar (2015) studied the onset of instability for Hagen–Poiseuille flow through tube with deformable walls and found that the scalings predicted by theory (using the neo-Hookean model) and experiments do not agree. However, a recent study by Verma & Kumaran (2015) has argued that it is more appropriate to consider the stability of the flow in the deformed configuration, as there is a non-negligible alteration of the shape of the deformable tube/channel due to the applied pressure gradient. By accounting for this modified base flow profile in the stability analysis, they found that the agreement between theory and experiments improved.

The studies discussed above used the old L2 formulation (with some inconsistencies, as discussed later in the manuscript) but Chokshi & Kumaran (2007, 2008*a*,*b*), introduced a modified Lagrangian formulation while studying the weakly nonlinear stability of plane Couette flow past a neo-Hookean solid, referred henceforth as 'L3' where 'L' and '3' stand respectively for Lagrangian and the number of states relevant in the formulation while carrying out the stability analysis. The three states that are important in the L3 formulation are the undeformed state, pre-stressed state (deformed base state) and the perturbed state similar to the L2 formulation used in previous works (Gkanis & Kumar 2003; Gaurav & Shankar 2009, 2010) but the L3 formulation uses the pre-stressed state as the reference state. We demonstrate that the L3 formulation of Chokshi & Kumaran (2007) is inconsistent as the base state (pre-stressed state) quantities were left as functions of undeformed coordinates, while the perturbed state quantities were functions of pre-stressed state coordinates. However, consistency demands that the base state quantities must be functions of the pre-stressed state coordinates.

Further, Chokshi & Kumaran (2008*a*,*b*) introduced an Eulerian formulation to study the stability of plane Couette flow of a viscoelastic fluid past a neo-Hookean solid. They also showed that the results predicted by using their Eulerian formulation agreed with the results from their L3 formulation both for linear and weakly nonlinear stability of plane Couette flow of a Newtonian fluid past a neo-Hookean solid for two-dimensional perturbations in the creeping-flow limit. Henceforth, we refer to the Eulerian formulation of Chokshi & Kumaran (2007) as 'Eulerian (CK)'. The neo-Hookean constitutive model in the Eulerian (CK) formulation appears to have been proposed in analogy with the constitutive relation for a Newtonian fluid, rather than by using the strain-energy function appropriate to the neo-Hookean solid, as is the standard practice in solid mechanics (Macosko 1994; Holzapfel 2000). It must be noted that for the neo-Hookean solid (in the Lagrangian formulation), the strain-energy function is a function of only the first invariant of the left Cauchy–Green tensor (Malvern 1969; Holzapfel 2000). However, we show in this paper that the purported Eulerian (neo-Hookean) constitutive relation proposed by Chokshi & Kumaran (2008*a*,*b*) assumes the strain energy as a function of only the second invariant of the left Cauchy–Green tensor (Holzapfel 2000). Thus, the nonlinear constitutive model used by (Chokshi & Kumaran 2008*a*,*b*) is really not the

conventional neo-Hookean model (Macosko 1994; Holzapfel 2000), but is in fact a special case of the Mooney–Rivlin constitutive model.

In this connection, there is a rather direct analogy with the development of constitutive relations for polymer solutions (Bird, Armstrong & Hassager 1977; Larson 1988), wherein purely on continuum grounds, there are two admissible constitutive relations, *viz*., upper-convected Maxwell (and Oldroyd-B with solvent contribution) and lower-convected Maxwell (and Oldroyd-A with solvent) models. However, experiments and molecular theories tend to support the upper-convected Maxwell/Oldroyd-B model. It can be shown that the use of the constitutive relation proposed by Chokshi & Kumaran (2008*a*) for the deformable solid is akin to the use of lower-convected Maxwell/Oldroyd-A model for polymer solutions. It can thus be expected that the results from neo-Hookean constitutive model for Eulerian (CK) formulation (Chokshi & Kumaran 2008*a*) need not necessarily agree with their L3 formulation. We demonstrate this by using the Eulerian (CK) formulation proposed by Chokshi & Kumaran (2008*a*) for the stability analysis of the plane Couette flow past a neo-Hookean surface and Hagen–Poiseuille flow through a neo-Hookean tube. Our analysis reveals, unexpectedly, that the results from the L3 and Eulerian (CK) formulations agree exactly for plane Couette flow (as also shown in Chokshi & Kumaran (2008*a*)), but this conclusion turns out to be a fortuitous coincidence for this specific geometry. In marked contrast, for Hagen–Poiseuille flow, the Eulerian (CK) formulation predicts a finite-wave instability which contradicts the predictions obtained by using L3 formulation. To resolve this, we propose a (consistent) Eulerian form for the neo-Hookean constitutive relation. In the absence of the strain-energy function as a function of current coordinates, we use the relation between deformation gradients in Lagrangian and Eulerian formulations to arrive at the alternative form of the neo-Hookean constitutive model in the Eulerian framework. Using this consistent Eulerian formulation of the neo-Hookean constitutive relation, we show that the results from the stability analyses (using the proposed Lagrangian L2 and L3, and Eulerian) are in exact agreement, thus demonstrating, for the first time, the consistency of the linear stability results for Hagen–Poiseuille flow in a neo-Hookean tube across various formulations.

The rest of this paper is structured as follows: the neo-Hookean constitutive relation in the Lagrangian formulation and its application to L3 formulation in general and for Hagen–Poiseuille flow in a neo-Hookean tube in particular are presented in § 2.1. In § 2.2 the proposed Eulerian formulation is discussed in which we outline general procedure to solve the stability problem of flow past a neo-Hookean solid using the proposed consistent neo-Hookean model in Eulerian frame of reference. We apply the proposed Eulerian formulation to the stability of Hagen–Poiseuille through a neo-Hookean tube in § 2.2. The results obtained by using Lagrangian (L2 and L3) and Eulerian (Eulerian (CK) and the proposed Eulerian) formulations for plane Couette flow past a neo-Hookean solid and Hagen–Poiseuille through a neo-Hookean tube in creeping-flow limit are presented in § 3.1. Section 3.2 discusses the effect of finite *Re*, i.e. the presence of inertial terms in both the fluid and solid, on the agreement among various formulations. The effect of including solid dissipation in the L2 and L3 formulations is presented in § 3.3. The salient conclusions of this work are presented in § 4. The Eulerian (CK) formulation for Hagen–Poiseuille flow through a neo-Hookean tube is presented in appendix A. A consistent approach to obtain linearized interface boundary conditions for the L3 formulation is outlined in appendix B. In appendix C, we provide the linearized perturbation equations in the L3 formulation for plane Couette flow past a neo-Hookean solid.

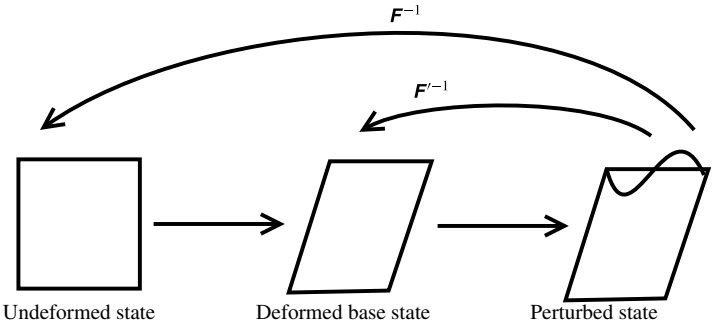


FIGURE 1. The undeformed ($\boldsymbol{X}$), pre-stressed ($\bar{\boldsymbol{x}}$), and perturbed ($\boldsymbol{x}$) states of the solid: initially the solid is in the undeformed state; upon imposition of the velocity field in the fluid creates a deformation in the solid to give rise to the pre-stressed base state. After imposition of perturbations, the solid will be in the perturbed state. The tensors $\boldsymbol{F}$ and $\boldsymbol{F}'$ are defined in the text.

## 2. Problem formulation

We consider two canonical unidirectional shear flows to illustrate our proposed formulation, *viz.*, plane Couette flow past a neo-Hookean solid, and Hagen–Poiseuille flow through a neo-Hookean tube. Before presenting the governing equations for these flows, we first introduce the L3 formulation implemented in the subsequent discussion. A generic schematic representation of the three states of the solid is shown in figure 1 which is relevant for the different formulations discussed in this paper.

### 2.1. *Lagrangian three state (L3) formulation*

Our formulation closely resembles the 'small-on-large theory' of nonlinear elasticity (Toupin & Bernstein 1961; Norris 2007) which involves the imposition of infinitesimal perturbations on a pre-stressed solid, and subsequent analysis of the dynamics of these perturbations. The use of small-on-large theory for studying wave motion in coupled fluid–solid systems is also prevalent in the theory of acoustoelasticity (Toupin & Bernstein 1961; Norris 2007) where it is used to study the evolution of acoustic perturbations superposed on a pre-stressed solid. Norris (2007) utilized this framework to calculate the wave speed in granular materials and fluid/solid systems, where the linear elastic model was used to investigate the evolution of disturbances. In the present work, however, we use the neo-Hookean model for the solid.

The formulation presented below builds upon the work of Chokshi & Kumaran (2008*a*), but with an important modification to remove an inconsistency in the earlier formulation discussed in detail below. Before proceeding to derive the base state and linearized perturbation equations, in the next subsection, we briefly recapitulate the derivation of the neo-Hookean constitutive relation in the Lagrangian formulation, which is applicable to both L2 and L3 formulations.

#### 2.1.1. *Neo–Hookean constitutive model*

We consider a representative particle in the solid with position vector $\boldsymbol{X}$, which changes to $\boldsymbol{x}$ because of a well-defined motion which relates $\boldsymbol{X}$ and $\boldsymbol{x}$. The two-point tensor which maps $\boldsymbol{X}$ to $\boldsymbol{x}$ is called the deformation gradient $\boldsymbol{F}$ defined as

(Malvern 1969; Holzapfel 2000)

$$\boldsymbol{F} = \frac{\partial \boldsymbol{x}}{\partial \boldsymbol{X}}. \tag{2.1}$$

In the present work we employ the following convention for the matrix elements of the deformation gradient tensor:

$$\boldsymbol{F} = \begin{bmatrix} \dfrac{\partial x_1}{\partial X_1} & \dfrac{\partial x_1}{\partial X_2} & \dfrac{\partial x_1}{\partial X_3} \\ \dfrac{\partial x_2}{\partial X_1} & \dfrac{\partial x_2}{\partial X_2} & \dfrac{\partial x_2}{\partial X_3} \\ \dfrac{\partial x_3}{\partial X_1} & \dfrac{\partial x_3}{\partial X_2} & \dfrac{\partial x_3}{\partial X_3} \end{bmatrix}. \tag{2.2}$$

Some authors (e.g. Larson 1999) use the transpose of the above matrix to represent the deformation gradient. In that case (the present) $\boldsymbol{F}$ in the constitutive equations must be replaced by (their) $\boldsymbol{F}^{\mathrm{T}}$ for consistency. Malvern (1969) uses the left operator $\overleftarrow{\nabla}$ to define above deformation gradient (2.2) while, the right operator $\overrightarrow{\nabla}$ is used to define the transpose of the above deformation gradient.

We assume an isotropic, incompressible, hyperelastic or Green-elastic material (Holzapfel 2000), i.e. a material for which strain-energy function $\psi$ exists. In the Lagrangian formulation for such a material, the Cauchy stress tensor $\boldsymbol{\sigma}$ is expressed in terms of the 'Finger' tensor (also referred to as the 'left Cauchy–Green' tensor), $\boldsymbol{b} = \boldsymbol{F} \cdot \boldsymbol{F}^{\mathrm{T}}$ and the strain-energy function $\psi$ as (Holzapfel 2000):

$$\boldsymbol{\sigma} = -p_g \boldsymbol{I} + 2\frac{\partial \psi(I_1, I_2)}{\partial I_1}\boldsymbol{b} - 2\frac{\partial \psi(I_1, I_2)}{\partial I_2}\boldsymbol{b}^{-1}, \tag{2.3}$$

where $I_1$ and $I_2$ are the first and second invariants of the tensor $\boldsymbol{b}$ and $p_g$ is pressure field in the solid. For a Mooney–Rivlin solid, the strain-energy function is a linear function of $I_1$ and $I_2$ (Macosko 1994; Holzapfel 2000)

$$\psi(I_1, I_2) = C_1 I_1 + C_2 I_2, \tag{2.4}$$

where $C_1$ and $C_2$ are the Mooney–Rivlin constants. Substituting the above equation in (2.3), we obtain

$$\boldsymbol{\sigma} = -p_g \boldsymbol{I} + 2C_1 \boldsymbol{b} - 2C_2 \boldsymbol{b}^{-1}. \tag{2.5}$$

In order to be consistent with the linear elastic model for small deformations the shear modulus of the material is $G = 2(C_1 + C_2)$ (Holzapfel 2000). For a neo-Hookean solid, the strain-energy function is (Macosko 1994):

$$\psi(I_1, I_2) = \tfrac{1}{2} G I_1, \tag{2.6}$$

where $G$ is the shear modulus of the solid. Substituting (2.6) in (2.3) and using the relation between the deformation gradient and $\boldsymbol{b}$, we obtain

$$\boldsymbol{\sigma} = -p_g \boldsymbol{I} + G\boldsymbol{F} \cdot \boldsymbol{F}^{\mathrm{T}}. \tag{2.7}$$

The above relation is the neo-Hookean constitutive model expressed in the Lagrangian formulation. Some authors (e.g. Larson 1999) use the transpose of the matrix (2.2) to denote $\boldsymbol{F}$, and in their convention, the neo-Hookean constitutive model will have a Cauchy stress tensor proportional to $\boldsymbol{F}^{\mathrm{T}}\boldsymbol{F}$, eventually yielding the same matrix

elements for the Cauchy stress tensor. From a molecular view point, the theory of rubber elasticity shows that the Cauchy stress tensor is a function of $\boldsymbol{b}$ (Larson 1999). Thus, the construction of the neo-Hookean constitutive relation is unambiguous with the prescription of the appropriate strain-energy function.

2.1.2. *Base state*

We consider a solid which is initially in its undeformed state, and denote a material particle with the position vector, $\boldsymbol{X} = (X_1, X_2, X_3)$. On this undeformed solid, a stress field is imposed by means of the fluid flowing past it. The continuity of the tangential and normal stress at the fluid–solid interface leads to a deformation field in the solid. We assume that the displacement in the solid due to fluid flow is only in the flow direction in the base state. The representative material particle will now assume a position vector, $\bar{\boldsymbol{x}} = (\bar{x}_1, \bar{x}_2, \bar{x}_3)$. The current position vector, $\bar{\boldsymbol{x}}$, and the position vector in the undeformed configuration $\boldsymbol{X}$ are related by

$$\bar{\boldsymbol{x}}(\boldsymbol{X}) = \boldsymbol{X} + \bar{\boldsymbol{u}}(\boldsymbol{X}), \tag{2.8}$$

where $\bar{\boldsymbol{u}}(\boldsymbol{X})$ is the Lagrangian displacement in the solid from undeformed state. To obtain the base (pre-stressed) state quantities, it is necessary to solve the momentum balance equations in the solid. The solid is assumed to be incompressible, and the incompressibility condition is given by $\det(\bar{\boldsymbol{F}}) = 1$ where, $\bar{\boldsymbol{F}} = \partial\bar{\boldsymbol{x}}/\partial\boldsymbol{X}$ is the base state deformation gradient. Here, an overbar is used to denote the base state quantities. The Cauchy stress in the base state for a neo-Hookean solid is

$$\bar{\boldsymbol{\sigma}} = -\bar{p}_g\boldsymbol{I} + G\bar{\boldsymbol{F}}\cdot\bar{\boldsymbol{F}}^{\mathrm{T}}, \tag{2.9}$$

with $\bar{p}_g$ being the pressure field in the solid in the base state. The momentum balance equation in the solid under steady base state conditions is (Malvern 1969; Holzapfel 2000),

$$\nabla_X\cdot\bar{\boldsymbol{P}} = 0, \tag{2.10}$$

where $\bar{\boldsymbol{P}}$ is the first Piola–Kirchoff stress tensor which is related to the Cauchy stress tensor $\bar{\boldsymbol{\sigma}}$ as (Malvern 1969) $\bar{\boldsymbol{P}} = \bar{\boldsymbol{F}}^{-1}\cdot\bar{\boldsymbol{\sigma}}$. It must be noted that some authors (e.g. Holzapfel 2000) define the first Piola–Kirchoff stress tensor as the transpose of the above definition. In that case, the momentum equation (2.10) would include the transpose of their first Piola–Kirchoff tensor (Holzapfel 2000) such that the eventual governing differential equations are identical. Assuming that the neo-Hookean solid is perfectly bonded to a rigid wall at a distance equal to the thickness of the deformable solid from the fluid–solid interface, we impose zero normal and tangential displacements at the rigid boundary. This implies

$$\bar{\boldsymbol{u}} = 0. \tag{2.11}$$

At the fluid–solid interface, the tangential and normal stress continuity conditions are needed to obtain the expressions for $\bar{\boldsymbol{u}}$ and $\bar{p}_g$.

2.1.3. *Perturbed state*

We impose infinitesimal perturbations on the above pre-stressed state, and track the same representative material particle in order to study the response of the coupled system to perturbations. After imposing perturbations, the material particle has the position $\boldsymbol{x} = (x_1, x_2, x_3)$. The relation between the pre-stressed state and the current position vector is

$$\boldsymbol{x}(\bar{\boldsymbol{x}}) = \bar{\boldsymbol{x}} + \boldsymbol{u}'(\bar{\boldsymbol{x}}, t), \tag{2.12}$$

where $\boldsymbol{u}'(\bar{\boldsymbol{x}})$ is the Lagrangian displacement of the particle from its pre-stressed state. The overall deformation gradient is a two-point tensor which maps particle positions from the undeformed state to the current state, and has following form

$$\boldsymbol{F} = \frac{\partial \boldsymbol{x}}{\partial \boldsymbol{X}} = \frac{\partial \boldsymbol{x}}{\partial \bar{\boldsymbol{x}}} \cdot \frac{\partial \bar{\boldsymbol{x}}}{\partial \boldsymbol{X}} = \boldsymbol{F}' \cdot \bar{\boldsymbol{F}}, \tag{2.13}$$

where $\boldsymbol{F}'$ is the perturbed state deformation gradient. Upon using the multiplicative property of determinants and the incompressibility condition for the base state, the incompressibility condition for the perturbed state becomes $\det(\boldsymbol{F}') = 1$. The Cauchy stress tensor for a neo-Hookean solid with viscous dissipation is (Holzapfel 2000; Destarde & Saccomandi 2004; Ma & Ng 2009; Giribabu & Shankar 2016),

$$\boldsymbol{\sigma} = -p_g \boldsymbol{I} + G\boldsymbol{F} \cdot \boldsymbol{F}^{\mathrm{T}} + \eta_g(\boldsymbol{L} + \boldsymbol{L}^{\mathrm{T}}), \tag{2.14}$$

where $p_g = \bar{p}_g + p'_g$, $p'_g$ is the perturbation to the pressure, $\boldsymbol{L} = \dot{\boldsymbol{F}} \cdot \boldsymbol{F}^{-1}$ is the spatial velocity gradient and $\eta_g$ is the viscosity of the neo-Hookean solid.

To define the first Piola–Kirchoff stress tensor, it must be noted that the reference configuration here is the pre-stressed state and it is necessary to take the dot product of the Cauchy stress tensor with an appropriate tensor which maps the current area to the pre-stressed area. This mapping is accomplished by the tensor $\boldsymbol{F}'^{-1}$. In contrast, for the L2 formulation, the dot product of the Cauchy stress tensor with $\boldsymbol{F}^{-1}$ is taken so that the resulting first Piola–Kirchoff stress tensor can be interpreted as the current force acting per undeformed state area. This is illustrated schematically in figure 1. Therefore the first Piola–Kirchoff tensor defined with respect to the pre-stressed state as the reference state is given by (Chokshi & Kumaran 2008*a*)

$$\boldsymbol{P} = \boldsymbol{F}'^{-1} \cdot \boldsymbol{\sigma}. \tag{2.15}$$

The momentum balance equation in terms of the first Piola–Kirchoff stress tensor is given by

$$\rho \frac{\partial^2 \boldsymbol{u}}{\partial t^2} = \nabla_{\bar{\boldsymbol{x}}} \cdot \boldsymbol{P}, \tag{2.16}$$

where $\rho$ is the density of the solid. It must be noted that thus far in the formulation, the base state quantities are functions of the coordinates of the undeformed state, $\boldsymbol{X}$, of the material particle, while the momentum balance equation for perturbations is defined in terms of pre-stressed coordinates of the particle, $\bar{\boldsymbol{x}}$, which was also the case with the earlier work of Chokshi & Kumaran (2008*a*). If the base state quantities are left as such in the analysis, then while deriving the linearized momentum equations, the presence of base state quantities creates an inconsistency. Therefore, in order to maintain consistency with respect to independent variables in the momentum balance equation, it is necessary to convert the base state quantities from being functions of undeformed state coordinates to functions of the pre-stressed state coordinates. This is illustrated below by considering the specific case of Hagen–Poiseuille flow in a deformable neo-Hookean tube.

2.1.4. *Hagen–Poiseuille flow*

We consider an incompressible Newtonian fluid with density $\rho$ and viscosity $\eta$ flowing through a tube of radius $R_t$ which lies in domain $0 \leqslant r \leqslant R_t$ with deformable walls from $r = R_t$ to $r = R_t(1 + H)$. We consider the same geometry as was used by Gaurav & Shankar (2009) for studying the temporal stability problem for Hagen–Poiseuille flow through a neo-Hookean tube. We non-dimensionalize lengths, velocity, pressure and stresses with respect to the radius of the tube $R_t$, $GR_t/\eta$ and $G$, respectively. In the ensuing discussion, for the sake of brevity, the non-dimensional dynamical variables are denoted without any superscript. The continuity equation for the fluid is

$$\boldsymbol{\nabla} \cdot \boldsymbol{v} = 0. \tag{2.17}$$

The Navier–Stokes equations take the form

$$\frac{Re}{\Gamma}\left(\frac{\partial \boldsymbol{v}}{\partial t} + (\boldsymbol{v} \cdot \boldsymbol{\nabla})\boldsymbol{v}\right) = -\boldsymbol{\nabla} p + \nabla^2 \boldsymbol{v}, \tag{2.18}$$

where, $p$ is pressure in the fluid, $Re = \rho R_t V/\eta$ is Reynolds number and $\Gamma = \eta V/GR_t$, is the dimensionless velocity with $V$ as the maximum velocity of the fluid in the base state. The base state velocity profile is the fully developed pressure-driven Hagen–Poiseuille flow in the tube

$$\bar{v}_z = \Gamma(1 - r^2). \tag{2.19}$$

To obtain the base state in the solid, we assume that the displacement in the solid occurs only in the flow direction in the base state. While experiments have shown that there is a variation of the tube diameter in the flow direction (Verma & Kumaran 2012), and hence the presence of a non-zero displacement in the radial direction, the magnitude of this radial displacement can be assumed to be small for the following reason. The pressure drop in the flow direction causes non-uniform displacement in the radial direction, leading to the variation of the tube diameter in the flow direction. The magnitude of the response (i.e. the radial displacement) will be determined by the non-dimensional strain in the solid, which is proportional to $\Gamma$ (Verma & Kumaran 2012). The pressure drop increases with increase in $Re$, hence the variation in the tube diameter along the flow direction will also increase with $Re$. At low $Re$, the variation of tube diameter is small (due to smaller pressure drops), and hence even for high values of $\Gamma$ the deformation in the radial direction will be much smaller in comparison with the tangential deformation. Similarly, at high $Re$ radial deformation becomes higher, but the critical $\Gamma$ value ($\Gamma_c$) for which flow becomes temporally unstable also decreases according to $\Gamma \sim Re^{-1/3}$ for wall modes and $\Gamma \sim Re^{-1}$ for inviscid modes (Gaurav & Shankar 2009). Due to such low values of $\Gamma$ the radial deformation will be much smaller in comparison with the tangential deformation. Thus, in both low and high Reynolds number regimes, the radial deformation of the solid in the base state can be assumed to be small when compared to the deformation in the flow direction. The governing equations for the perturbed state in dimensionless form are

$$\det(\boldsymbol{F}') = 1, \tag{2.20}$$

$$\frac{Re}{\Gamma}\frac{\partial^2 \boldsymbol{u}}{\partial t^2} = \boldsymbol{\nabla}_{\bar{\boldsymbol{x}}} \cdot \boldsymbol{P}, \tag{2.21}$$

$$\boldsymbol{\sigma} = -p_g \boldsymbol{I} + \boldsymbol{F} \cdot \boldsymbol{F}^{\mathrm{T}} + \eta_r(\boldsymbol{L} + \boldsymbol{L}^{\mathrm{T}}), \tag{2.22}$$

where $\eta_r = \eta_g/\eta$. Following the procedure outlined in § 2.1.2, we define a motion which maps a representative material particle from the undeformed state to the deformed base state

$$\bar{r}(R) = R, \tag{2.23}$$

$$\bar{z}(R, Z) = Z + \bar{u}_z(R). \tag{2.24}$$

Following § 2.1.2 we obtain the following expressions for solid deformation in the base state

$$\bar{u}_z(R) = \Gamma((1+H)^2 - R^2), \quad \bar{u}_r = \bar{u}_\theta = 0, \tag{2.25a,b}$$

and the pressure $\bar{p}_g(R, Z)$, for solid in the base state is obtained after using the normal stress continuity boundary condition at the fluid–solid interface:

$$\bar{p}_g(R, Z) = -4\Gamma Z + 4\Gamma^2(R^2 - 1) = -4\Gamma Z + 4\Gamma^2(R^2 - 1). \tag{2.26}$$

Here the independent variables are the coordinates in the undeformed state. The above results are identical to those of Gaurav & Shankar (2009), as the procedure is same. As mentioned at the end of the previous section, we next convert the base state quantities as a function of variables in the pre-stressed state. Equations (2.23) and (2.24) can also be written in following form,

$$R(\bar{r}) = \bar{r}, \tag{2.27}$$

$$Z(\bar{r}, \bar{z}) = \bar{z} - \bar{u}_z(\bar{r}). \tag{2.28}$$

Using the above inverted form for motion the base state quantities can be expressed in terms of pre-stressed state variables

$$\bar{u}_z(\bar{r}) = \Gamma((1+H)^2 - \bar{r}^2), \quad \bar{u}_r = \bar{u}_\theta = 0, \tag{2.29a,b}$$

$$\bar{p}_g(\bar{z}) = -4\Gamma\bar{z} + \alpha, \tag{2.30}$$

where $\alpha$ is a constant of integration. Comparison of (2.26) and (2.30) for pressure shows the independence of $\bar{p}_g$ on $\bar{r}$ which is a major point of departure from the L2 formulation of Gaurav & Shankar (2009). It must be noted that this difference arises because of the different reference frames and does not affect the results of the stability analysis.

The above change of variables can also be accomplished by directly substituting (2.27) and (2.28) in (2.26) to obtain,

$$\bar{p}_g(\bar{z}) = -4\Gamma\bar{z} + 4\Gamma^2(H^2 + 2H). \tag{2.31}$$

Comparing (2.30) and (2.31) we obtain, $\alpha = 4\Gamma^2(1+H)^2 - 4\Gamma^2$, which confirms the consistency of our mathematical formulation. Equations (2.29) and (2.30) are then used to derive the Cauchy stress tensor in the base state

$$\boldsymbol{\sigma} = \begin{bmatrix} 1+4\Gamma\bar{z} & 0 & -2\Gamma\bar{r} \\ 0 & 1+4\Gamma\bar{z} & 0 \\ -2\Gamma\bar{r} & 0 & 1+4\Gamma\bar{z}+4\Gamma^2\bar{r}^2 \end{bmatrix}. \tag{2.32}$$

The first and second normal stress differences are, $\sigma_{zz}-\sigma_{rr}=4\Gamma^2\bar{r}^2$ and $\sigma_{rr}-\sigma_{\theta\theta}=0$, respectively. On the above base state, infinitesimal axisymmetric perturbations are now imposed. The normal modes for the quantities on the fluid side are,

$$(v_r', v_z', p')(\boldsymbol{x}, t) = (\mathrm{i}\tilde{v}_r, \tilde{v}_z, \tilde{p})(r)\mathrm{e}^{\mathrm{i}k(z-ct)}, \tag{2.33}$$

and for the variables on the solid side are,

$$(u_r', u_z', p_g')(\bar{\boldsymbol{x}}, t) = (\mathrm{i}\tilde{u}_r, \tilde{u}_z, \tilde{p}_g)(\bar{r})\mathrm{e}^{\mathrm{i}k(\bar{z}-ct)}, \tag{2.34}$$

where, $k$ is wavenumber in axial direction while $c=c_r+\mathrm{i}c_i$ is the complex velocity of perturbations. Therefore the flow becomes temporally unstable if $c_i>0$. The governing equations for the fluid after linearization are

$$k\,\tilde{v}_z+\frac{\tilde{v}_r}{r}+\mathrm{D}\tilde{v}_r=0, \tag{2.35}$$

$$-\mathrm{D}\tilde{p}+\mathrm{i}\left(\mathrm{D}^2+\frac{1}{r}\mathrm{D}-\frac{1}{r^2}-k^2\right)\tilde{v}_r=-\frac{Re}{\Gamma}[k\tilde{v}_r(\bar{v}_z-c)], \tag{2.36}$$

$$-\mathrm{i}k\tilde{p}+\left(\mathrm{D}^2+\frac{1}{r}\mathrm{D}-k^2\right)\tilde{v}_z=\mathrm{i}\frac{Re}{\Gamma}[k\tilde{v}_z(\bar{v}_z-c)+\mathrm{D}\bar{v}_z\tilde{v}_r], \tag{2.37}$$

where, $\mathrm{D}=\mathrm{d}/\mathrm{d}r$. Similarly, for the solid, the continuity equation is given by

$$k\,\tilde{u}_z+\frac{\tilde{u}_r}{\bar{r}}+\mathrm{D}\tilde{u}_r=0, \tag{2.38}$$

and the linearized momentum equations are given by

$$\begin{aligned}-\mathrm{D}\tilde{p}_g+4\Gamma k\tilde{u}_r-4\Gamma\,\mathrm{D}\tilde{u}_z+\mathrm{i}(1-\mathrm{i}kc\eta_r)\left(\mathrm{D}^2+\frac{1}{\bar{r}}\mathrm{D}-\frac{1}{\bar{r}^2}-k^2\right)\tilde{u}_r\\ -(-4\Gamma k\bar{r}\,\mathrm{D}+4\mathrm{i}\Gamma^2k^2\bar{r}^2)\tilde{u}_r=-\mathrm{i}k^2c^2\frac{Re}{\Gamma}\tilde{u}_r,\end{aligned} \tag{2.39}$$

$$\begin{aligned}-\mathrm{i}kp_g-4\mathrm{i}\Gamma k\tilde{u}_z+4\mathrm{i}\Gamma\left(\frac{1}{\bar{r}}+\mathrm{D}\right)\tilde{u}_r+(1-\mathrm{i}kc\eta_r)\left(\mathrm{D}^2+\frac{1}{\bar{r}}\mathrm{D}-k^2\right)\tilde{u}_z\\ -(4\mathrm{i}\Gamma k\bar{r}\,\mathrm{D}+4\Gamma^2k^2\bar{r}^2)\tilde{u}_z=-k^2c^2\frac{Re}{\Gamma}\tilde{u}_z,\end{aligned} \tag{2.40}$$

here $\mathrm{D}=\mathrm{d}/\mathrm{d}\bar{r}$. The above linearized governing equations are subject to the following boundary conditions. At $r=0$, the symmetry conditions are applicable at the centre of the tube:

$$\tilde{v}_r=0,\quad \mathrm{D}\tilde{v}_z=0. \tag{2.41a,b}$$

At $r=1$, we use the linearized interface conditions at the fluid–solid interface. To derive interface conditions, it is necessary to Taylor expand the base state quantities of the fluid, because the solid is described in the Lagrangian frame of reference (material particle has same label, irrespective of the state) while the fluid is described in the Eulerian frame of reference. Gkanis & Kumar (2005) Taylor expanded the base state quantities for both the fluid and solid while studying the linear stability analysis of plane Poiseuille flow through a neo-Hookean channel and predicted

finite-wave instability in creeping-flow limit. Later Gaurav & Shankar (2010) studied the same problem but Taylor expanded only the fluid side base state quantities and found that the finite-wave instability in the creeping-flow limit is absent. Lee *et al.* (2014), while studying gravity-driven instability of a thin liquid film underneath a soft solid, observed that if the solid is to be described in terms of Eulerian variables (upon transformation from Lagrangian variables), the interface conditions are not straightforward to derive. It must be noted that in the present work the deformable solid is described using both Lagrangian and Eulerian frames of reference and will be treated as such while solving the problem without inter-conversion of the quantities. Hence here, the ambiguity does not arise while deriving the interface conditions.

The disagreement between the predictions of Gkanis & Kumar (2005) and Gaurav & Shankar (2010) shows the importance of incorporating consistent interface conditions. In the present work, we show (see appendix B) that the base state quantities of the fluid side should be Taylor expanded in both the flow direction ($z$) and the normal direction to the flow ($r$) unlike in the case of Gaurav & Shankar (2010) where they had Taylor expanded the base state quantities of the fluid only in the normal direction to the flow ($r$). It must be noted that in addition to the normal direction, a Taylor expansion of the fluid (base state) quantities is also needed in the flow direction in order to cancel out all the base state terms in the fluid and solid at the interface. The derivation of the linearized conditions in the L3 formulation is discussed at length in appendix B of this paper and the consequences of the Taylor expansion in both (flow and normal) directions on the stability of various flows will be addressed separately in a subsequent work. Here we give the final forms of the linearized continuity conditions at $r = 1$

$$\tilde{v}_r = -\mathrm{i}kc\tilde{u}_r, \tag{2.42}$$

$$\tilde{v}_z - 2\mathrm{i}\Gamma\tilde{u}_r = -\mathrm{i}kc\tilde{u}_z, \tag{2.43}$$

$$\mathrm{D}\tilde{v}_z - k\tilde{v}_r = -2\mathrm{i}\Gamma k\tilde{u}_z - 2\mathrm{i}\Gamma\,\mathrm{D}\tilde{u}_r + 2\mathrm{i}\Gamma\tilde{u}_r + (1 - \mathrm{i}kc\eta_r)(\mathrm{D}\tilde{u}_z - k\tilde{u}_r), \tag{2.44}$$

$$-\tilde{p} + 2\mathrm{i}\,\mathrm{D}\tilde{v}_r = -\tilde{p}_g + 2\mathrm{i}(1 - \mathrm{i}kc\eta_r)\,\mathrm{D}\tilde{u}_r + 4\Gamma k\tilde{u}_r - 4\Gamma\tilde{u}_z. \tag{2.45}$$

Comparison of (2.38)–(2.40) and the above interface conditions for the solid with the linearized differential equations and interface conditions of Gaurav & Shankar (2009) shows the difference in the manner in which interaction of the base state with the perturbations manifest themselves in the two formulations. The most important difference arises in the continuity equation, because there is no interaction term in the L3 formulation unlike in the old L2 formulation of Gaurav & Shankar (2009). This is due to the fact that the material frame of reference in the case of Gaurav & Shankar (2009) is the undeformed state, while in the present case it is the pre-stressed state. This change in reference frame should not, however, affect the conclusions made regarding the stability of the system. Also both frames are separated by a distance $\bar{u}_z(r)$, hence the displacements in the two formulations could be different but the velocities will not be different as neither frame is moving relative to the other. However, for interface conditions the difference arises not only because of the Taylor expansion of both fluid and solid base state quantities by Gaurav & Shankar (2009) in the $r$ direction but also because of the different frames of reference.

At $r = 1 + H$, we enforce zero radial and horizontal displacements as the neo-Hookean solid is assumed to be fixed to the rigid wall, which implies

$$\tilde{u}_r = 0, \quad \tilde{u}_z = 0. \tag{2.46a,b}$$

The governing equations and the above boundary conditions are solved for the eigenvalue $c$ using both numerical integration combined with shooting and pseudospectral (Boyd 2001) methods.

### 2.2. *Eulerian formulation*

The Eulerian formulation used here follows closely the procedure outlined in the work of Chokshi & Kumaran (2008*a*,*b*). However the principles used to arrive at the proposed neo-Hookean model are different from the development of the Eulerian (CK) formulation (see appendix A) as explained below.

#### 2.2.1. *Neo-Hookean constitutive model*

The deformation gradient for the Eulerian formulation is (Malvern 1969; Chokshi & Kumaran 2008*a*) $\boldsymbol{f} = \partial \boldsymbol{X}/\partial \boldsymbol{x}$. A comparison of this relation with (2.1) leads to the relation between deformation gradients in the Eulerian and Lagrangian formulations

$$\boldsymbol{F} = \boldsymbol{f}^{-1}. \tag{2.47}$$

To derive the neo-Hookean model as in the case of the Lagrangian formulation (see § 2.1.1) we lack a strain energy function in solid mechanics literature for the Eulerian framework, i.e. strain-energy function as a function of the current coordinates. Instead we observe that some authors (Norris 2008) have circumvented the problem of the non-existence of strain energy in the Eulerian formulation by using alternative relations which uses the definition of mechanical power and the rate of work per unit current volume of the material, to arrive at Eulerian conjugate stress and strain. This idea of using conjugate stress and strain in Eulerian formulation is a cumbersome mathematical procedure.

However, the uniqueness of Cauchy stress tensor can be utilized here to derive the neo-Hookean equation in the Eulerian formulation by using mathematical relation (2.47) directly in (2.7) to obtain (in non-dimensional form)

$$\boldsymbol{\sigma} = -p_g \boldsymbol{I} + (\boldsymbol{f}^{\mathrm{T}} \cdot \boldsymbol{f})^{-1}. \tag{2.48}$$

#### 2.2.2. *Base state*

To obtain the equations of motion, we assume that initially the solid is in the undeformed state. The base state deformation gradient is

$$\bar{\boldsymbol{f}} = \frac{\partial \boldsymbol{X}}{\partial \boldsymbol{x}}. \tag{2.49}$$

The incompressibility condition is (Chokshi & Kumaran 2008*a*,*b*) $\det(\bar{\boldsymbol{f}}) = 1$. The relation between the position of the particle in the deformed and undeformed configuration is,

$$\boldsymbol{x} = \boldsymbol{X} + \bar{\boldsymbol{u}}(\boldsymbol{x}), \tag{2.50}$$

here $\bar{\boldsymbol{u}}(\boldsymbol{x})$ is the Eulerian base state displacement in the solid. The Cauchy stress for the base state by using (2.48) is

$$\bar{\boldsymbol{\sigma}} = -\bar{p}_g \boldsymbol{I} + (\bar{\boldsymbol{f}}^{\mathrm{T}} \cdot \bar{\boldsymbol{f}})^{-1}. \tag{2.51}$$

By using the above definition of the Cauchy stress tensor, the momentum balance equation for the steady base state is (Malvern 1969; Chokshi & Kumaran 2008*a*)

$$\boldsymbol{\nabla}_{\boldsymbol{x}} \cdot \bar{\boldsymbol{\sigma}} = 0. \tag{2.52}$$

After solving the governing equations for deformation $\bar{\boldsymbol{u}}(\boldsymbol{x})$ and $\bar{p}_g$, the interface conditions (velocity and stress balance) at $r = 1$ and at $r = 1 + H$, boundary condition (2.11) is to be used to obtain expressions for $\bar{\boldsymbol{u}}(\boldsymbol{x})$ and $\bar{p}_g$.

2.2.3. *Perturbed state*

We next impose perturbations on the above base state and track the representative particle, which now has the position vector $\boldsymbol{x} = (x_1, x_2, x_3)$ and is related to $\boldsymbol{X}$ by following relation

$$\boldsymbol{x} = \boldsymbol{X} + \bar{\boldsymbol{u}}(\boldsymbol{x}) + \boldsymbol{u}'(\boldsymbol{x}, t), \tag{2.53}$$

here $\bar{\boldsymbol{u}}'(\boldsymbol{x}, t)$ is the Eulerian perturbed state displacement in the solid. Hence for the perturbed state the deformation gradient modifies to $\boldsymbol{f} = \partial \boldsymbol{X}/\partial \boldsymbol{x}$. The non-dimensional Cauchy momentum balance becomes

$$\frac{Re}{\Gamma}\left(\frac{\partial \boldsymbol{v}^g}{\partial t} + (\boldsymbol{v}^g \cdot \nabla_x)\boldsymbol{v}^g\right) = \nabla_x \cdot \boldsymbol{\sigma}, \tag{2.54}$$

where $\boldsymbol{v}^g$ is the velocity in the solid and is related to the displacement in the solid by the relation (Chokshi & Kumaran 2008*a*),

$$\boldsymbol{v}^g = \frac{\partial \boldsymbol{u}}{\partial t} + \boldsymbol{v}^g \cdot \frac{\partial \boldsymbol{u}}{\partial \boldsymbol{x}}. \tag{2.55}$$

The above methodology is used for the stability analysis of the Hagen–Poiseuille flow and is discussed next.

2.2.4. *Hagen–Poiseuille flow*

Following the procedure outlined in the previous two sections, the base state deformation and pressure are,

$$\bar{u}_z(r) = \Gamma\,[(1+H)^2 - r^2], \tag{2.56}$$

$$\bar{p}_g(z) = \bar{p}(z) = -4\Gamma z. \tag{2.57}$$

Using above base state deformation and pressure we obtain the Cauchy stress tensor in the base state

$$\boldsymbol{\sigma} = \begin{bmatrix} 1+4\Gamma z & 0 & -2\Gamma r \\ 0 & 1+4\Gamma z & 0 \\ -2\Gamma r & 0 & 1+4\Gamma z+4\Gamma^2 r^2 \end{bmatrix}. \tag{2.58}$$

The first and second normal stress differences are, $\sigma_{zz} - \sigma_{rr} = 4\Gamma^2 r^2$ and $\sigma_{rr} - \sigma_{\theta\theta} = 0$, respectively. Comparing (2.32) and (2.58) we find that the base state Cauchy stress tensor is identical for Eulerian and L3 formulations, with the identification of $\bar{\boldsymbol{x}}$ as the current coordinate in the L3 formulation in the base state.

On the above base state, infinitesimal axisymmetric perturbations are imposed to study the stability of the coupled system. These perturbations are then substituted in (2.54) and then these equations are linearized. The fluid side governing equations for perturbations will be same as given in § 2.1.4. For the solid, the normal modes are taken of the form,

$$(u_r', u_z', p_g')(\boldsymbol{x}, t) = (\mathrm{i}\tilde{u}_r, \tilde{u}_z, \tilde{p}_g)(r)\mathrm{e}^{\mathrm{i}k(z-ct)}. \tag{2.59}$$

The governing equations for the solid after substitution of normal modes become,

$$k\tilde{u}_z + \frac{\tilde{u}_r}{r} + \mathrm{D}\tilde{u}_r - 2\mathrm{i}\Gamma k\tilde{u}_r = 0, \tag{2.60}$$

$$\mathrm{i}\mathrm{D}\tilde{p}_g + \left(\mathrm{D}^2 - 2\mathrm{i}k\Gamma r\,\mathrm{D} + \frac{1}{r}\mathrm{D} - \frac{1}{r^2} - k^2 - 2\mathrm{i}k\Gamma\right)\tilde{u}_r + 2\mathrm{i}k^2\Gamma r\tilde{u}_z = -k^2c^2\frac{Re}{\Gamma}\tilde{u}_r, \tag{2.61}$$

$$-\mathrm{i}k\tilde{p}_g + \left(\mathrm{D}^2 - 2\mathrm{i}k\Gamma r\,\mathrm{D} + \frac{1}{r}\mathrm{D} - k^2 + 4\mathrm{i}k\Gamma\right)\tilde{u}_z + \left(4\mathrm{i}\Gamma\,\mathrm{D} + 2\mathrm{i}k^2\Gamma r + 8k\Gamma^2 r + \frac{4\mathrm{i}\Gamma}{r}\right)\tilde{u}_r = -k^2c^2\frac{Re}{\Gamma}\tilde{u}_z + 2\mathrm{i}\Gamma k^2c^2\frac{Re}{\Gamma}r\tilde{u}_r, \tag{2.62}$$

where, $\mathrm{D} = \mathrm{d}/\mathrm{d}r$. A comparison of above equations with (2.38)–(2.40) shows the difference in the interaction of the base state quantities with the perturbed state quantities which arises because of the different frames of references.

Equations (2.35)–(2.37) for the fluid and (2.60)–(2.62) for the solid must be solved with the following boundary conditions. At the tube centre, (2.41) is applicable. At $r = 1$, the linearized fluid–solid interface conditions are

$$\tilde{v}_r = -\mathrm{i}kc\tilde{u}_r, \tag{2.63}$$

$$\tilde{v}_z - 2\mathrm{i}\Gamma\tilde{u}_r = -\mathrm{i}kc\tilde{u}_z + 2\Gamma kc\tilde{u}_r, \tag{2.64}$$

$$\mathrm{D}\tilde{v}_z - k\tilde{v}_r = 4\Gamma^2k\tilde{u}_r + \mathrm{D}\tilde{u}_z + 2\mathrm{i}\Gamma k\tilde{u}_z - k\tilde{u}_r + 4\mathrm{i}\Gamma\tilde{u}_r, \tag{2.65}$$

$$-\tilde{p} + 2\mathrm{i}\,\mathrm{D}\tilde{v}_r = -\tilde{p}_g - 2\mathrm{i}k\tilde{u}_z - 2\mathrm{i}\tilde{u}_r. \tag{2.66}$$

At $r = 1 + H$, zero vertical or horizontal displacement conditions are applicable as neo-Hookean solid is fixed to rigid solid, which implies,

$$\tilde{u}_r = 0, \quad \tilde{u}_z = 0. \tag{2.67a,b}$$

## 3. Results and discussion

### 3.1. *Creeping-flow limit*

#### 3.1.1. *Plane Couette flow*

In order to compare the two Lagrangian (L2 and L3) and Eulerian (Eulerian (CK) and the proposed Eulerian) formulations for predicting the stability of the coupled neo-Hookean solid–fluid system, we compare the eigenvalues obtained from all the formulations for the same set of parameters. For plane Couette flow past a neo-Hookean solid the results of both the Eulerian (CK) formulation and the L3 formulation described above agree in the creeping-flow limit. Appendix C discusses the derivation of the linearized governing equations for plane Couette flow in the L3 formulation. Table 1 shows the most unstable (or least stable) eigenvalue for the plane Couette flow case for different parameters for all the four formulations, and the results from all the four formulations agree very well. Here $\Gamma = \eta V/GL$, with $V$ the velocity of the top plate and $L$ the thickness of the fluid layer.

To demonstrate the agreement for a range of $k$ values, the real and imaginary parts of most unstable (or least stable) eigenvalue are plotted in figure 2 for different parameter values. The instabilities shown in the figure 2 at $k \sim 0.1$ and high $k$ ($k \sim O(10)$) are finite-wave and short-wave instabilities respectively. From table 1 and figure 2, the agreement is exact up to the third decimal place as observed in the work of Chokshi & Kumaran (2008*a*). It must be noted that eigenvalues shown

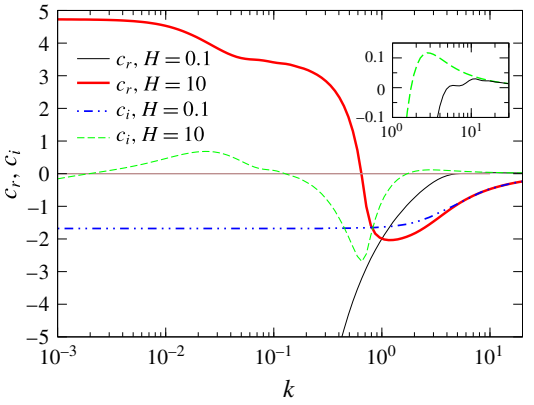


FIGURE 2. (Colour online) The variation of $c_r$ and $c_i$ with $k$ for $\Gamma = 10$, $H = 0.1$, 10, $Re = 0$, $\eta_r = 0$ for Couette flow, using all the four formulations. The results are identical for all the formulations, and hence the same legend is used to represent the results. The inset ($c_i$ versus $k$) demonstrates the instability at high wavenumbers.

| Parameters | $k$ | Eulerian (CK) | Eulerian, L2 and L3 |
|---|---|---|---|
| $H = 0.1$, $\Gamma = 1$ | 1 | $-0.15841 - 2.1015$i | $-0.15841 - 2.1015$i |
| $H = 0.1$, $\Gamma = 1$ | 10 | $-0.00394 - 0.09130$i | $-0.00394 - 0.09130$i |
| $H = 0.1$, $\Gamma = 10$ | 10 | $-0.46638 + 0.02765$i | $-0.46638 + 0.02763$i |
| $H = 1$, $\Gamma = 10$ | 10 | $-0.47333 + 0.04084$i | $-0.47333 + 0.04084$i |
| $H = 10$, $\Gamma = 10$ | 0.1 | $3.4091 + 0.09960$i | $3.4092 + 0.09963$i |

TABLE 1. Eigenvalues obtained from the Eulerian and Lagrangian formulations for Couette flow for different parameters. Data show agreement between Eulerian and Lagrangian formulations for $Re = 0$, $\eta_r = 0$.

in the work of Gkanis & Kumar (2003), where they have used old L2 formulation, also show exact agreement with the L3 formulation and hence is grouped with the Eulerian and L3 formulations in the last column of table 1. It must be noted that the old L2 and L2 formulations turn out to be same for plane Couette flow owing to the simplicity of the flow geometry, thus leading to exact agreement for this geometry.

We next demonstrate that the agreement between the proposed Eulerian and Eulerian (CK) formulation observed above, is quite general for a planar flow geometry subjected to two-dimensional perturbations. For planar shear flows that are under consideration, the most general form of the deformation gradient is

$$\boldsymbol{f} = \begin{bmatrix} 1 - \partial_x u'_x & -d_y \bar{u}_x - \partial_y u'_x \\ -\partial_x u'_y & 1 - \partial_y u'_y \end{bmatrix}, \tag{3.1}$$

where $d_y \bar{u}_x$ is the base state deformation gradient with $x$ as flow direction and $y$ as direction perpendicular to the flow which could, in general function of $y$ (plane Poiseuille flow). Substituting $\boldsymbol{f}$ in (A 1) the linearized Cauchy stress tensor ($\boldsymbol{\sigma}^c$) in Eulerian (CK) formulation becomes

$$\boldsymbol{\sigma}^c = \begin{bmatrix} -p'_g + 2\partial_x u'_x & \partial_y u'_x + \partial_x u'_y - \partial_x u'_x d_y \bar{u}_x \\ \partial_y u'_x + \partial_x u'_y - \partial_x u'_x d_y \bar{u}_x & -p'_g + 2\partial_y u'_y - 2\partial_y u'_x d_y \bar{u}_x \end{bmatrix}. \tag{3.2}$$

It must be noted that the identity tensor in (A 1) has been absorbed in $p_g$ to facilitate the comparison. Using the above definition of Cauchy stress tensor and normal modes (2.59) in (2.54) (with $Re = 0$) and elimination of perturbation pressure from the resulting momentum balance equations we obtain the final equation

$$\begin{aligned} &d_y^4\tilde{u}_y + 2\mathrm{i}kd_y\bar{u}_x d_y^3\tilde{u}_y + (-2k^2 - k^2(d_y\bar{u}_x)^2 + 3\mathrm{i}kd_y^2\bar{u}_x)d_y^2\tilde{u}_y \\ &\quad + (-2\mathrm{i}k^3 d_y\bar{u}_x - 2k^2 d_y\bar{u}_x d_y^2\bar{u}_x + 2\mathrm{i}kd_y^3\bar{u}_x)d_y\tilde{u}_y \\ &\quad + (k^4 + k^4(d_y\bar{u}_x)^2 - \mathrm{i}k^3 d_y^2\bar{u}_x + \mathrm{i}kd_y^4\bar{u}_x)\tilde{u}_y = 0. \end{aligned} \tag{3.3}$$

To compare the proposed Eulerian formulation we substitute $\boldsymbol{f}$ in (2.48), to obtain the linearized Cauchy stress tensor for the proposed Eulerian formulation as

$$\boldsymbol{\sigma} = \begin{bmatrix} -p_g' - 2\partial_y u_y' + 2d_y\bar{u}_x\partial_y u_x' & \partial_y u_x' + \partial_x u_y' - d_y\bar{u}_x\partial_x u_x' \\ \partial_y u_x' + \partial_x u_y' - d_y\bar{u}_x\partial_x u_x' & -p_g' - 2\partial_x u_x' \end{bmatrix}. \tag{3.4}$$

It can be shown that by adopting the same procedure (as has been done for the Eulerian (CK) formulation) to the above stress tensor, we again obtain (3.3), thereby showing that the fourth-order differential equation is identical for both the formulations. It is also necessary to show the equivalence of interface conditions for different formulations but in the interest of brevity here we demonstrate only the normal stress continuity at the fluid–solid interface. For the proposed Eulerian formulation:

$$-p_g' - 2\partial_x u_x' = -p_f' + 2\partial_y v_y'. \tag{3.5}$$

Substituting $u_x'$ from continuity equation, $p_g'$ from $x$-momentum balance equation for the proposed Eulerian formulation and normal modes we obtain

$$\begin{aligned} &2\mathrm{i}k\tilde{u}_y d_y\bar{u}_x + 3d_y\tilde{u}_y - (d_y\bar{u}_x)^2 d_y\tilde{u}_y - \frac{\mathrm{i}}{k}d_y^2\bar{u}_x d_y\tilde{u}_y - \frac{2\mathrm{i}}{k}d_y\bar{u}_x d_y^2\tilde{u}_y - \frac{\mathrm{i}}{k}d_y^3\bar{u}_x\tilde{u}_y \\ &\quad = -\tilde{p}_f + 2d_y\tilde{v}_y. \end{aligned} \tag{3.6}$$

For the Eulerian (CK) formulation:

$$-p_g' + 2\partial_y u_y' - 2d_y\bar{u}_x\partial_x u_y' = -p_f' + 2\partial_y v_y'. \tag{3.7}$$

By substituting for pressure $p_g'$ from the $x$-momentum equation, we again obtain (3.6), thereby proving the equivalence of both the Eulerian formulations for planar flows. This agreement, however, holds only for the planar flows subjected to two-dimensional perturbations under creeping flow because of the rather simple structure of the matrix $\boldsymbol{f}^{\mathrm{T}} \cdot \boldsymbol{f}$ for two-dimensional perturbations. For three-dimensional perturbations the rather complicated form of the $\boldsymbol{f}^{\mathrm{T}} \cdot \boldsymbol{f}$ tensor gives rise to a very different $(\boldsymbol{f}^{\mathrm{T}} \cdot \boldsymbol{f})^{-1}$ which can potentially lead to disagreement between two formulations for three-dimensional perturbations.

### 3.1.2. *Hagen–Poiseuille flow*

Gaurav & Shankar (2009) used inconsistent interface conditions while studying stability of the Hagen–Poiseuille flow through a neo-Hookean tube as they Taylor expanded both fluid and solid sides while deriving interface conditions. The discussion in § 2.1.4 regarding interface conditions is applicable for the L2 formulation as well,

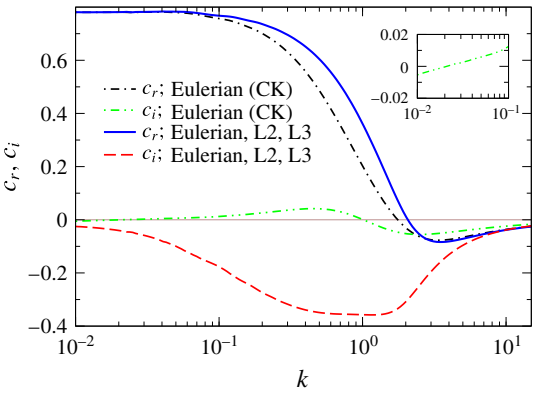


FIGURE 3. (Colour online) The variation of $c_r$ and $c_i$ with $k$ for parameters $\Gamma = 0.8$, $H = 10$, $Re = 0$, $\eta_r = 0$ for Hagen–Poiseuille flow for four formulations. Eulerian, L2 and L3 formulations agree, but Eulerian (CK) formulation disagrees as it shows the presence of finite-wave instability. The inset ($c_i$ versus $k$) demonstrates the transition from stable to unstable region at low wavenumbers.

| Parameters | $k$ | Eulerian (CK) | Eulerian, L2, and L3 |
|---|---|---|---|
| $H = 0.1$, $\Gamma = 1$ | 1 | $-0.32988 - 2.0559$i | $-0.32984 - 2.0598$i |
| $H = 0.1$, $\Gamma = 1$ | 10 | $-0.02919 - 0.05522$i | $-0.02831 - 0.06473$i |
| $H = 0.1$, $\Gamma = 10$ | 20 | $-0.49209 + 0.02464$i | $-0.49229 + 0.01870$i |
| $H = 1$, $\Gamma = 10$ | 10 | $-0.98067 + 0.05380$i | $-0.98149 + 0.03033$i |
| $H = 10$, $\Gamma = 0.8$ | 0.1 | $0.75715 + 0.01248$i | $0.76767 - 0.17670$i |
| $H = 10$, $\Gamma = 10$ | 0.1 | $0.65674 + 1.5400$i | $4.5876 - 12.672$i |

TABLE 2. Eigenvalues predicted by Eulerian and Lagrangian formulations for Hagen–Poiseuille flow for different parameters. The last two columns show lack of agreement between Eulerian and Lagrangian formulations for $Re = 0$, $\eta_r = 0$. The results are obtained using both shooting and pseudospectral methods.

i.e. only fluid side quantities must be Taylor expanded in both flow and normal directions. The consequences of this modification on the stability of the flow for different parameters will be discussed in a subsequent work. Here we compare all the four formulations by using the most unstable (or the least stable) eigenvalues for different parameters as shown in table 2, which indicate that unlike in the case of plane Couette flow, the eigenvalues obtained by using the Eulerian (CK) formulation do not agree with the eigenvalues found by using Eulerian, L2 or L3 formulations.

To understand the differences more clearly for different values of $k$, the real and imaginary parts of the most unstable (or the least stable) eigenvalues are plotted in figure 3. It is readily observed from figure 3 that there is disagreement in the prediction of the instability between Eulerian (CK) and the other three formulations. The largest difference is for the finite-wave instability predicted by Eulerian (CK) formulation, which is absent in the work of Gaurav & Shankar (2009) as well but the proposed Eulerian formulation does not predict finite-wave instability in creeping-flow limit. Also the eigenvalues predicted by the proposed Eulerian, L2 and L3 formulations agree as shown in the table 2. To illustrate the differences between Eulerian (CK) and L3 formulations, in figure 4, we plot the variation of $c_r$ and $c_i$

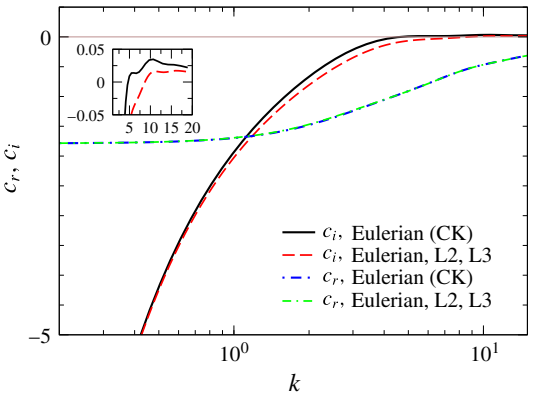


FIGURE 4. (Colour online) The variation of $c_r$ and $c_i$ with $k$ for parameters $\Gamma = 5$, $H = 0.1$, $Re = 0$, $\eta_r = 0$ for Hagen–Poiseuille flow using Eulerian (CK), Eulerian, L2 and L3 formulations. The eigenvalues obtained by using Eulerian (CK) and L3 formulations disagree but for Eulerian, L2 and L3 formulations the agreement is observed. The inset ($c_i$ versus $k$) demonstrates the instability at high wavenumbers.

with respect to $k$ for parameter values $H = 0.1$, $\Gamma = 5$ for both formulations which shows that the quantitative difference (in terms of critical parameters $\Gamma_c$, $k_c$) still exists even for low $H$ values where only short-wave (high $k$) instability is present. From figure 4 we can also see that as we increase $k$, the Eulerian (CK) and L3 formulations tend to agree but from table 2, this agreement is only up to the first or second decimal place. In the inset of figure 4 the difference becomes evident.

It must be noted that the presence of finite-wave instability for Hagen–Poiseuille flow through a linear viscoelastic tube in the creeping-flow limit was predicted by Kumaran (1995*b*) and this was shown to occur for $\Gamma > O(1)$. However, the linear viscoelastic model is valid only for $\Gamma \ll 1$ as elaborated by Gaurav & Shankar (2009) because for $\Gamma > O(1)$ finite deformation coupling terms become important, which makes the nonlinear terms in the strain tensor important.

The uniqueness of the Cauchy stress tensor requires that the Eulerian and Lagrangian frames of reference should predict the same eigenvalues for same parameter values. The agreement between the proposed Eulerian and L3 formulations confirms the Galilean frame invariance of the neo-Hookean model. But from figures 3 and 4 it is clear that the Eulerian (CK) formulation does not agree with the Eulerian formulation used in the present work with respect to prediction of the eigenvalues which also uses an Eulerian frame of reference. This suggests that there could be a problem with one of the formulations as discussed below. The neo-Hookean model for Lagrangian description is derived from a well-defined strain-energy function as discussed in § 2.1.1 and the agreement of results predicted by using L3 formulation with the results produced by using Eulerian formulation (mathematically equivalent to Lagrangian neo-Hookean model, see § 2.2) shows that the neo-Hookean model in Lagrangian formulation is indeed frame invariant. This is further reinforced from the agreement observed with the results of Gaurav & Shankar (2009) and the present work which demonstrates the Galilean frame-invariant nature of the Lagrangian formulation. It must be noted that both formulations are Lagrangian descriptions, but the frames of reference are different.

It is shown in appendix A.1 that the neo-Hookean constitutive equation used in Eulerian (CK) formulation is in fact a special case of the Mooney–Rivlin model (2.5)

with $C_1 = 0$ and $C_2 = \frac{1}{2}G$, hence the Eulerian (CK) constitutive model is not really the true neo-Hookean model. This suggests that the results obtained by using Eulerian (CK) formulation might not agree with the L3 formulation. The results presented in table 2 and figure 3 confirm that the hypothesis is indeed correct and the Eulerian (CK) formulation does not agree with the L3 formulation in general.

Similar to the case of plane Couette flow discussed above, we attempt to examine the agreement between Eulerian (CK) and the proposed Eulerian formulations for a general case of flow through a tube. For axisymmetric perturbations for flow through a neo-Hookean tube, the deformation gradient tensor is

$$\boldsymbol{f} = \begin{bmatrix} 1 - \partial_r u_r' & 0 & -\partial_z u_r' \\ 0 & 1 - \dfrac{u_r'}{r} & 0 \\ -d_r\bar{u}_z - \partial_r u_z' & 0 & 1 - \partial_z u_z' \end{bmatrix}, \tag{3.8}$$

where $d_r\bar{u}_z$ is the base state deformation gradient. Substituting $\boldsymbol{f}$ in (A 1) we obtain expression for the linearized Cauchy stress tensor in the Eulerian (CK) formulation

$$\boldsymbol{\sigma}^c = \begin{bmatrix} -p_g' + 2\partial_r u_r' - 2d_r\bar{u}_z\partial_r u_z' & 0 & \partial_z u_r' + \partial_r u_z' + d_r\bar{u}_z\partial_z u_z' \\ 0 & -p_g' + 2\dfrac{u_r'}{r} & 0 \\ \partial_z u_r' + \partial_r u_z' + d_r\bar{u}_z\partial_z u_z' & 0 & -p_g' + 2\partial_z u_z' \end{bmatrix}. \tag{3.9}$$

Using above expression for the Cauchy stress tensor in (2.54) (with $Re = 0$), the linearized momentum balance equations in the creeping-flow limit are obtained. The fourth-order differential equation, after eliminating pressure from the momentum balance equations, is

$$\begin{aligned} &\left(\frac{2}{r} + 2\mathrm{i}kd_r\bar{u}_z\right) d_r^3\tilde{u}_r + \left(-2k^2 - \frac{3}{r^2} + \frac{3\mathrm{i}k}{r}d_r\bar{u}_z - k^2(d_r\bar{u}_z)^2 + 3\mathrm{i}kd_r^2\bar{u}_z\right) d_r^2\tilde{u}_r \\ &\quad + \left(\frac{3}{r^3} - \frac{2k^2}{r} - 2\mathrm{i}k^3 d_r\bar{u}_z - \frac{\mathrm{i}k}{r^2}d_r\bar{u}_z - \frac{k^2}{r}(d_r\bar{u}_z)^2 + \frac{\mathrm{i}k}{r}d_r^2\bar{u}_z - 2k^2 d_r\bar{u}_z d_r^2\bar{u}_z\right) d_r\tilde{u}_r \\ &\quad + \left(2\mathrm{i}kd_r^3\bar{u}_z\right) d_r\tilde{u}_r + \left(k^4 - \frac{3}{r^4} + \frac{2k^2}{r^2} + \frac{2\mathrm{i}k}{r^3}d_r\bar{u}_z - \frac{\mathrm{i}k^3}{r}d_r\bar{u}_z + k^4(d_r\bar{u}_z)^2\right)\tilde{u}_r \\ &\quad + \left(-\frac{k^2}{r^2}(d_r\bar{u}_z)^2 - \mathrm{i}k^3 d_r^2\bar{u}_z - \frac{2\mathrm{i}k}{r^2}d_r^2\bar{u}_z + \mathrm{i}kd_r^4\bar{u}_z\right)\tilde{u}_r + d_r^4\tilde{u}_r = 0. \end{aligned} \tag{3.10}$$

Similarly substituting $\boldsymbol{f}$ in (2.48) the linearized Cauchy stress tensor for the proposed Eulerian formulation is

$$\boldsymbol{\sigma} = \begin{bmatrix} -p_g' - 2\dfrac{u_r'}{r} - \partial_z u_z' & 0 & -2\dfrac{u_r'}{r}d_r\bar{u}_z + \partial_z u_r' - d_r\bar{u}_z\partial_z u_z' + \partial_r u_z' \\ 0 & -p_g' + 2\dfrac{u_r'}{r} & 0 \\ -2\dfrac{u_r'}{r}d_z\bar{u}_z + \partial_z u_r' - d_z\bar{u}_z\partial_z u_z' + \partial_r u_z' & 0 & -p_g' - 2(1 + (d_r\bar{u}_z)^2)\dfrac{u_r'}{r} - 2\partial_r u_r' + 2d_r\bar{u}_z\partial_r u_z' \end{bmatrix}. \tag{3.11}$$

Hence the fourth-order differential equation for the proposed Eulerian formulation is

$$\left(\frac{2}{r}+2\mathrm{i}kd_r\bar{u}_z\right)d_r^3\tilde{u}_r+\left(-2k^2-\frac{3}{r^2}+\frac{3\mathrm{i}k}{r}d_r\bar{u}_z-k^2(d_r\bar{u}_z)^2+3\mathrm{i}kd_r^2\bar{u}_z\right)d_r^2\tilde{u}_r$$
$$+\left(\frac{3}{r^3}-\frac{2k^2}{r}-2\mathrm{i}k^3d_r\bar{u}_z-\frac{5\mathrm{i}k}{r^2}d_r\bar{u}_z-\frac{k^2}{r}(d_r\bar{u}_z)^2\right)d_r\tilde{u}_r$$
$$+\left(\frac{5\mathrm{i}k}{r}d_r^2\bar{u}_z-2k^2d_r\bar{u}_zd_r^2\bar{u}_z+2\mathrm{i}kd_r^3\bar{u}_z\right)d_r\tilde{u}_r+\left(k^4-\frac{3}{r^4}+\frac{2k^2}{r^2}\right)\tilde{u}_r$$
$$+\left(\frac{4\mathrm{i}k}{r^3}d_r\bar{u}_z-\frac{\mathrm{i}k^3}{r}d_r\bar{u}_z+k^4(d_r\bar{u}_z)^2+\frac{k^2}{r^2}(d_r\bar{u}_z)^2-\mathrm{i}k^3d_r^2\bar{u}_z\right)\tilde{u}_r$$
$$+\left(-\mathrm{i}k^3d_r^2\bar{u}_z-\frac{4\mathrm{i}k}{r^2}d_r^2\bar{u}_z-\frac{2k^2}{r}d_r\bar{u}_zd_r^2\bar{u}_z+\frac{2\mathrm{i}k}{r}d_r^3\bar{u}_z+\mathrm{i}kd_r^4\bar{u}_z\right)\tilde{u}_r+d_r^4\tilde{u}_r=0. \quad (3.12)$$

Equations (3.10) and (3.12) show that for both the formulations the fourth-order differential equations are different and because of this reason the stability results for tube flow do not agree for both formulations even in creeping-flow limit which is in stark contrast to planar flows. Even the linearized interface conditions differ for the formulations. To illustrate this, we demonstrate here only the shear stress continuity at the interface. For Eulerian (CK) formulation the shear stress continuity at the fluid–solid interface gives

$$-(d_r\bar{u}_z)^2\partial_zu_r'+\partial_zu_r'+\partial_ru_z'-d_r\bar{u}_z\partial_zu_z'=\partial_zv_r'+\partial_rv_z'. \quad (3.13)$$

Substituting $u_z'$ from the incompressibility condition along with the normal modes in the above equation we obtain

$$\frac{1}{k}\tilde{u}_r-k\tilde{u}_r-\frac{1}{k}d_r\tilde{u}_r+\underline{\mathrm{i}\tilde{u}_rd_r\bar{u}_z}-\frac{1}{k}d_r^2\tilde{u}_r-\mathrm{i}\tilde{u}_rd_r^2\bar{u}_z=-k\tilde{v}_r+d_r\tilde{v}_z. \quad (3.14)$$

Similarly for the Eulerian formulation the shear stress balance at the interface gives

$$-(d_r\bar{u}_z)^2\partial_zu_r'-2d_r\bar{u}_zu_r'+\partial_zu_r'-d_r\bar{u}_z\partial_zu_z'+\partial_ru_z'=\partial_zv_r'+\partial_rv_z', \quad (3.15)$$

which upon use of the incompressibility condition to eliminate $u_z'$ results in the following equation

$$\frac{1}{k}\tilde{u}_r-k\tilde{u}_r-\frac{1}{k}d_r\tilde{u}_r+\underline{3\mathrm{i}\tilde{u}_rd_r\bar{u}_z}-\frac{1}{k}d_r^2\tilde{u}_r-\mathrm{i}\tilde{u}_rd_r^2\bar{u}_z=-k\tilde{v}_r+d_r\tilde{v}_z. \quad (3.16)$$

Comparison of (3.14) and (3.16) shows that, unlike in the case of planar flows, the interface conditions for the Eulerian (CK) and Eulerian formulations are not equivalent, hence the disagreement.

### 3.2. *Results at finite Re*

From the above discussion it is still not clear whether these conclusions in the creeping-flow limit are also applicable at finite *Re* when there is presence of an extra inertial term which interacts with the base state in $z$-momentum equation of the solid for the Eulerian formulations, as shown in (2.62) and (A 10). The plane Couette flow past a neo-Hookean solid also has a similar interaction term for the Eulerian (CK)

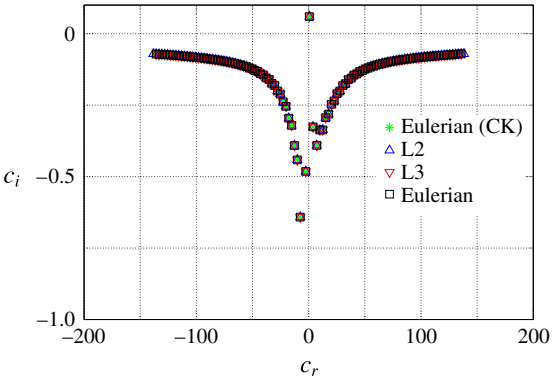


FIGURE 5. (Colour online) Eigenvalue spectrum in the $c_r$–$c_i$ plane for Eulerian (CK), Eulerian, L2 and L3 formulations for parameters $k = 0.5$, $\Gamma = 2$, $H = 5$, $Re = 0.5$, $\eta_r = 0$; for plane Couette flow. The spectra predicted by all four formulations show excellent agreement with each other.

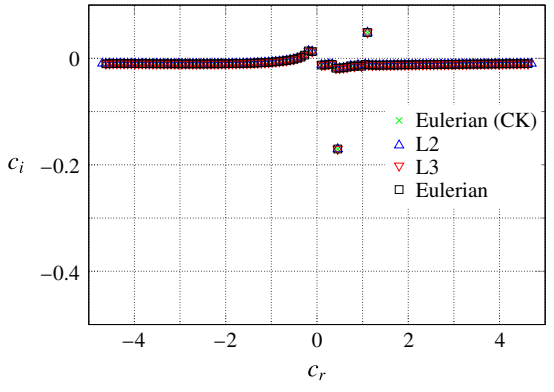


FIGURE 6. (Colour online) Eigenvalue spectrum in the $c_r$–$c_i$ plane for Eulerian (CK), Eulerian, L2 and L3 formulations for parameters $k = 0.5$, $\Gamma = 2$, $H = 5$, $Re = 500$, $\eta_r = 0$; for plane Couette flow. Figure confirms the agreement between the Lagrangian and Eulerian formulations at high $Re$.

formulation, as noted by Chokshi & Kumaran (2008*b*). Following the discussion of the creeping-flow limit results for plane Couette flow past a neo-Hookean solid, for non-zero $Re$ as well, we find that the results from all formulations agree. Figures 5 and 6 show agreement among the spectra for Eulerian (CK), Eulerian, L2 and L3 formulations for arbitrary $Re$.

Figure 7 shows the comparison of the proposed Eulerian, L2 and L3 spectra for Hagen–Poiseuille flow for parameters $k = 0.5$, $\Gamma = 2$, $H = 5$, $Re = 0.1$. All the three spectra overlap, showing conclusive evidence of agreement between the proposed Eulerian, L2 and L3 formulations for non-zero $Re$ as well. Similarly, figure 8 shows comparison of spectra obtained by using L3 and Eulerian (CK) formulations. From figure 8, the following important conclusions can be inferred: (i) the modes of instability for the L3 formulation are different from those of the Eulerian (CK) formulation; (ii) the finite-wave unstable mode found in the creeping-flow limit

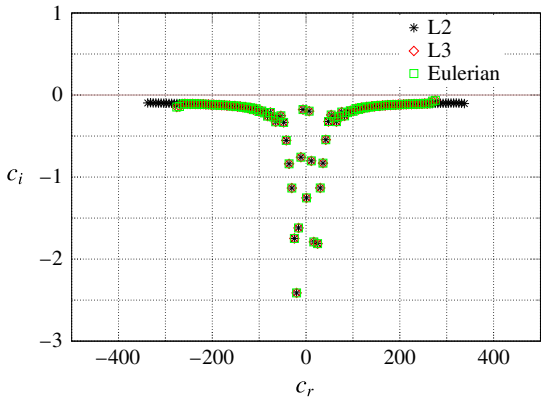


FIGURE 7. (Colour online) Eigenvalue spectrum in the $c_r$–$c_i$ plane for Eulerian, L2 and L3 formulations for parameters $k = 0.5$, $\Gamma = 2$, $H = 5$, $Re = 0.1$, $\eta_r = 0$ for Hagen–Poiseuille flow. Figure confirms agreement among Eulerian, L2 and L3 formulations.

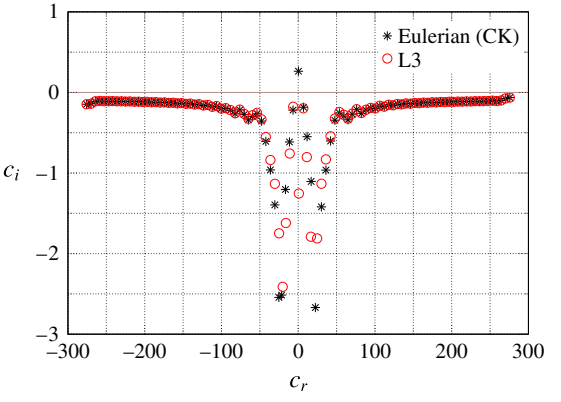


FIGURE 8. (Colour online) Eigenvalue spectrum in the $c_r$–$c_i$ plane for L3 and Eulerian (CK) formulations for parameters $k = 0.5$, $\Gamma = 2$, $H = 5$, $Re = 0.1$, $\eta_r = 0$; for Hagen–Poiseuille flow. There is disagreement between the Eulerian (CK) and L3 formulations, especially in the prediction of the unstable mode.

governs the stability behaviour for low $Re$ in the Eulerian (CK) formulation, but the finite-wave unstable mode is absent in the L3 formulation for low $Re$.

For low values of $\Gamma$, the spectra for both L3 and Eulerian (CK) formulations agree. This occurs because for low $\Gamma$, interaction terms (which are characteristic of any nonlinear solid model), between base state and perturbations become small and both formulations approach the linear viscoelastic model asymptotically. This is illustrated in figure 9 for parameters $Re = 100$, $H = 10$, $k = 0.5$, $\Gamma = 0.1$. As we increase $\Gamma$, results from both formulations start to differ as shown in figure 10 for parameters $Re = 100$, $H = 10$, $k = 0.5$, $\Gamma = 2$. At high $Re$ i.e. for $Re \sim 1000$ the inertial forces are dominant and hence agreement between Eulerian(CK) and L3 formulations can be observed even for higher values of $\Gamma$. Indeed as shown in figure 11, the difference between the eigenvalues predicted by using Eulerian (CK) and L3 formulation is of $O(10^{-3})$.

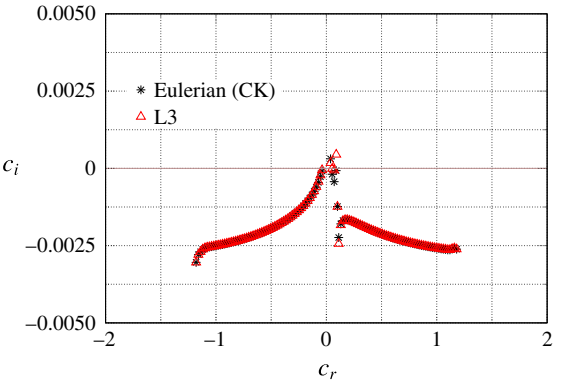


FIGURE 9. (Colour online) Spectra of Eulerian (CK) and L3 formulations for parameters $k = 0.5$, $\Gamma = 0.1$, $H = 10$, $Re = 100$, $\eta_r = 0$ for Hagen–Poiseuille flow. Figure shows reasonable agreement between Eulerian (CK) and L3 formulations for low $\Gamma$ where both formulations approach linear viscoelastic model asymptotically.

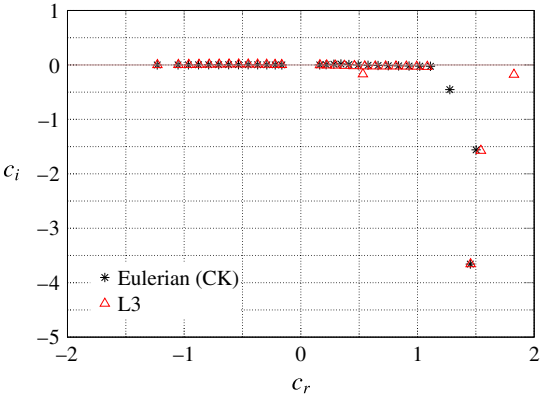


FIGURE 10. (Colour online) Eigenvalue spectrum in the $c_r$–$c_i$ for Eulerian (CK) and L3 formulations for parameters $k = 0.5$, $\Gamma = 2$, $H = 10$, $Re = 100$, $\eta_r = 0$ for Hagen–Poiseuille flow. Figure shows disagreement between Eulerian (CK) and L3 formulations as $\Gamma$ is increased.

### 3.3. *Results at finite Re and* $\eta_r \neq 0$

In this section we consider non-zero dissipation in the solid to examine the agreement between the L2 and L3 formulations so as to conclude the utility of the L3 formulation presented here to study hydrodynamic stability of flow past a neo-Hookean solid. Figure 12 shows spectra of the L2 and L3 formulations for Couette flow using parameter values $k = 0.5$, $\Gamma = 5$, $H = 5$, $Re = 0.5$, $\eta_r = 0.1$. The agreement between the results obtained by using L2 and L3 formulations is evident from figure 12 for Couette flow as both spectra overlap.

Gaurav & Shankar (2009), while studying stability analysis of Hagen–Poiseuille flow through a neo-Hookean tube, concluded that the viscous dissipation in the solid has a strong stabilizing effect on the upstream modes for low $Re$, but for high $Re$ there is little effect of $\eta_r$ on the stability of upstream modes. The spectrum for both formulations is plotted for parameters $k = 1$, $\Gamma = 3$, $H = 5$, $Re = 10$, $\eta_r = 0.1$ in figure 13

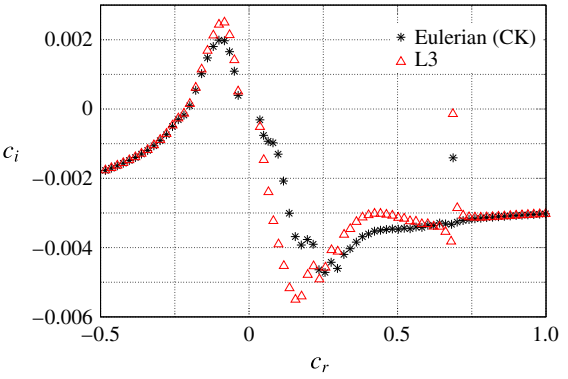


FIGURE 11. (Colour online) Eigenvalue spectrum in the $c_r$–$c_i$ plane for Eulerian (CK) and L3 formulations for parameters $k = 1$, $\Gamma = 1$, $H = 5$, $Re = 1000$, $\eta_r = 0$ for Hagen–Poiseuille flow. Figure shows substantial disagreement between Eulerian and L3 formulations even when inertial forces dominate the viscous forces.

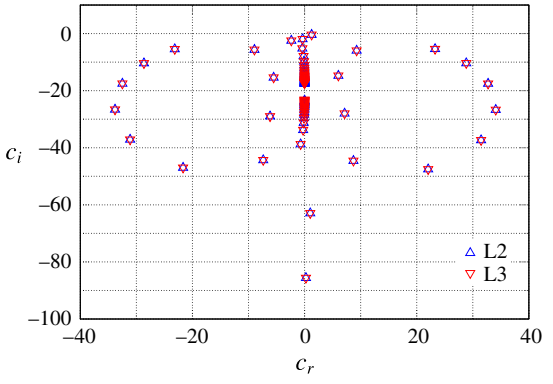


FIGURE 12. (Colour online) Spectra for L2 and L3 formulations for parameters $k = 0.5$, $\Gamma = 5$, $H = 5$, $Re = 0.5$, $\eta_r = 0.1$ for Couette flow. Figure confirms agreement between L2 and L3 formulations for $\eta_r \neq 0$.

which shows agreement between L2 and L3 formulations. This proves the utility of the L3 formulation to study stability of flows past a deformable surface.

## 4. Conclusions

In the present work, we introduced and demonstrated consistent formulations (both Eulerian and Lagrangian) to carry out stability analysis for flows past a neo-Hookean solid by considering the specific cases of plane Couette flow past a neo-Hookean solid and Hagen–Poiseuille flow through a neo-Hookean tube. Two types of Lagrangian formulations are considered here and they differ in the reference states assumed while formulating the problem. We modified the old L2 formulation by Taylor expanding the fluid quantities in both the flow and normal to the flow directions to make it consistent. Similarly, we proposed crucial modifications to make the L3 formulation (as described in Chokshi & Kumaran 2008*a*) consistent by means of transformation of variables. We show that this modified L3 formulation yields same result as consistent L2 formulation

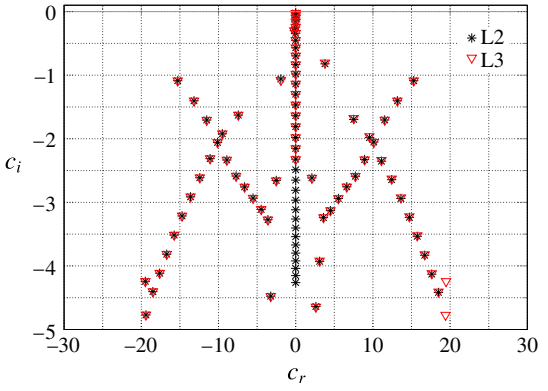


FIGURE 13. (Colour online) Spectra for L2 and L3 formulations for parameters $k = 1$, $\Gamma = 3$, $H = 5$, $Re = 10$, $\eta_r = 0.1$ for Hagen–Poiseuille flow. Figure confirms agreement between L2 and L3 formulations for non-zero $\eta_r$.

thus confirming the consistency of the two Lagrangian formulations. At the same time, we also show that the derivation of the linearized interface conditions is unambiguous in the L3 formulation unlike in the case of L2 formulation. We also demonstrated a crucial inconsistency in the Eulerian (CK) formulation which is attributed to the lack of a well-defined strain-energy function while deriving the neo-Hookean model in the Eulerian formulation as required by fundamental principles of continuum mechanics (Holzapfel 2000). It must be noted that the Cauchy stress tensor used in the work of Chokshi & Kumaran (2008*a*,*b*) was proposed in analogy with the Cauchy stress tensor of a Newtonian fluid, and as discussed in appendix A.1, the nonlinear solid model in the Eulerian (CK) formulation is in fact a special case of the Mooney–Rivlin model (2.5) and is not the neo-Hookean model.

This discrepancy prompted us to propose a consistent Eulerian formulation for the neo-Hookean solid. To circumvent the problem of the absence of strain-energy function in Eulerian formulation in deriving the neo-Hookean model, we used the mathematical relation $\boldsymbol{F} = \boldsymbol{f}^{-1}$ and proposed an alternative Eulerian formulation of the neo-Hookean constitutive model. The proposed model is then used for the stability analysis of the plane Couette flow past a neo-Hookean solid and Hagen–Poiseuille flow through a neo-Hookean tube. Comparison of the results (for Hagen–Poiseuille flow) obtained by using the consistent Eulerian and L3 formulations showed that the both formulations agree and, unlike in the case of the Eulerian (CK) formulation, the proposed Eulerian formulation does not exhibit a finite-wave instability in the creeping-flow limit. The agreement among Eulerian (CK), Eulerian, L2 and L3 formulations observed for plane Couette flow case is merely a coincidence, and as elaborated in § 3.1, in the creeping-flow limit, for planar flows, the fourth-order differential equations and linearized interface conditions in fact turn out to be mathematically equivalent for the Eulerian (CK) and the proposed Eulerian formulations, thus giving rise to the same eigenvalues. However, for Hagen–Poiseuille flow through a neo-Hookean tube, the fourth-order differential equation and the linearized interface conditions cannot be reduced to mathematically equivalent form for Eulerian (CK) and the proposed Eulerian formulations. We thus conclude that the nonlinear ('neo-Hookean') constitutive relation of Chokshi & Kumaran (2008*a*) in the Eulerian (CK) formulation does not agree with the L3 formulation for arbitrary flows.

Interestingly, a simple linear combination of (2.7) and (A 3) yields a special case of the Mooney–Rivlin model with $C_1 = C_2 = \frac{1}{2}G$. As noted above, the Eulerian (CK) formulation shows a finite-wave instability in the creeping-flow limit. This suggests that if the solid is modelled using the Mooney–Rivlin model, the Hagen–Poiseuille flow in a deformable tube might exhibit a finite-wave instability in the creeping-flow limit for appropriate values of the two constants. We further demonstrated the consistency between L2, L3 and the proposed Eulerian formulations at finite and high $Re$ for both flow geometries considered here. A comparison of spectra (at finite and high $Re$) between the L3 and Eulerian (CK) formulations in the $c_r$–$c_i$ plane shows the presence of different modes of instability with the number of unstable modes being different in the Eulerian (CK) compared to the L3/consistent Eulerian formulation.

The present work thus presents consistent methods for carrying out linear stability analyses for fluid flow past a neo-Hookean solid, and the consistency is demonstrated for two different flow geometries and for arbitrary Reynolds number. Our study shows that the stability of the flow in a deformable tube is very sensitive to the nature of the constitutive equation used for the solid, in marked contrast to plane Couette flow past a deformable solid where the qualitative features of the stability are quite robust at any $Re$. This conclusion makes an interesting contrast when juxtaposed with the stability characteristics of plane Couette flow and Hagen–Poiseuille flow with rigid walls, where both these flows share a lot of similarities with regard to linear stability (Drazin & Reid 1981; Schmid & Henningson 2001). Our work shows that for, deformable neo-Hookean solid walls, the stability features of plane Couette and Hagen–Poiseuille flows are drastically different, and geometry plays a crucial role in dictating the presence or absence of the instability in these flows when the wall is deformable.

## Acknowledgements

We would like to acknowledge instructive discussions on continuum mechanics with Dr A. Gupta, Department of Mechanical Engineering, Indian Institute of Technology Kanpur.

## Appendix A. Eulerian (CK) formulation

We briefly outline here the Eulerian formulation of Chokshi & Kumaran (2008*a*,*b*) for the case of flow in a tube.

### A.1. *Neo–Hookean constitutive model*

As explained in § 2.2, in the absence of a well-defined strain-energy function for Eulerian formulation, it is not possible to derive the neo-Hookean model in the Eulerian formulation. However, Chokshi & Kumaran (2008*a*) proposed a neo-Hookean model in analogy with the constitutive relation for a Newtonian fluid (P. Chokshi, personal communication) as,

$$\boldsymbol{\sigma} = -p_g \boldsymbol{I} + 2G\boldsymbol{e}, \tag{A 1}$$

$$\boldsymbol{e} = \tfrac{1}{2}(\boldsymbol{I} - \boldsymbol{f}^{\mathrm{T}} \cdot \boldsymbol{f}), \tag{A 2}$$

here $\boldsymbol{e}$ is the Eulerian strain tensor (Malvern 1969). To obtain the equivalent Lagrangian formulation of the Eulerian (CK) formulation using relation $\boldsymbol{f} = \boldsymbol{F}^{-1}$ in (A 1) and absorbing the identity tensor in the pressure term, we obtain

$$\boldsymbol{\sigma} = -p_g \boldsymbol{I} - G(\boldsymbol{F} \cdot \boldsymbol{F}^{\mathrm{T}})^{-1}. \tag{A 3}$$

The above constitutive relation can be obtained from (2.3) using the following strain-energy function

$$\psi(I_1, I_2) = \tfrac{1}{2} G I_2. \tag{A 4}$$

Substituting the above strain-energy function in (2.3) and using relation $\boldsymbol{b} = \boldsymbol{F} \cdot \boldsymbol{F}^{\mathrm{T}}$ we obtain (A 3). Equation (2.3) shows that the constitutive equation of Chokshi & Kumaran (2008*a*) is a nonlinear relation between $\boldsymbol{\sigma}$ and $\boldsymbol{b}$ and the 'neo-Hookean' model of the Chokshi & Kumaran (2008*a*,*b*) describes a hyperelastic solid with strain-energy function as a function of the second invariant of the left Cauchy–Green tensor, $\boldsymbol{b}$. But according to the fundamental definition of a neo-Hookean solid, the strain-energy function for such a solid is a function of only first invariant of the left Cauchy–Green tensor (Macosko 1994; Holzapfel 2000). This implies that the model used in Chokshi & Kumaran (2008*a*,*b*) is not what is conventionally referred to as the neo-Hookean model in solid mechanics. Also comparison of (2.5) and (A 3) shows that the Eulerian (CK) constitutive relation is in fact the Mooney–Rivlin model with $C_1 = 0$ and $C_2 = \frac{1}{2}G$.

The procedure to use the Eulerian (CK) formulation proposed by Chokshi & Kumaran (2008*a*,*b*) to solve the stability of flows past a soft solid is identical to the procedure outlined in § 2.2, but for the difference in the nature of the constitutive relation.

### A.2. *Hagen–Poiseuille flow*

We next analyse the stability of Hagen–Poiseuille flow in a deformable tube. Following the procedure in § 2.2, the base state deformation and pressure is,

$$\bar{u}_z = \Gamma[(1+H)^2 - r^2], \tag{A 5}$$

$$\bar{p}_g = \bar{p}(z) + 6\Gamma^2\left(\tfrac{1}{3} - r^2\right). \tag{A 6}$$

Using above base state deformation and pressure we obtain base state Cauchy stress tensor

$$\boldsymbol{\sigma} = \begin{bmatrix} 4\Gamma z - 6\Gamma^2\left(\frac{1}{3} - r^2\right) - 4\Gamma^2 r^2 & 0 & -2\Gamma r \\ 0 & 4\Gamma z - 6\Gamma^2\left(\frac{1}{3} - r^2\right) & 0 \\ -2\Gamma r & 0 & 4\Gamma z - 6\Gamma^2\left(\frac{1}{3} - r^2\right) \end{bmatrix}. \tag{A 7}$$

The first and second normal stress differences are, $\sigma_{zz} - \sigma_{rr} = 4\Gamma^2 r^2$ and $\sigma_{rr} - \sigma_{\theta\theta} = -4\Gamma^2 r^2$, respectively. Comparing (2.32), (2.2) and (A 7) leads to the conclusion that the Eulerian (CK) formulation has non-zero $\sigma_{rr} - \sigma_{\theta\theta}$ unlike the case of the Eulerian and L3 formulations. Also, comparison of (2.57) and (A 6) shows that $\bar{p}_g$ in the solid for the Eulerian (CK) formulation is a function of $r$ unlike in the case of the Eulerian formulation proposed in this work. Thus, the disagreement between the Eulerian (CK) and L3 formulations begins to appear even at the level of the base state, which is a consequence of the inconsistent neo-Hookean model in the Eulerian (CK) formulation. The linearized governing equations for the solid, after substitution of the normal modes, become

$$k\tilde{u}_z + \frac{\tilde{u}_r}{r} + \mathrm{D}\tilde{u}_r - 2\mathrm{i}\Gamma k\tilde{u}_r = 0, \tag{A 8}$$

$$-\mathrm{D}\tilde{p}_g + \mathrm{i}\left(2\,\mathrm{D}^2 + \frac{2\,\mathrm{D}}{r} - \frac{2}{r^2} - k^2\right)\tilde{u}_r + (4\Gamma r\,\mathrm{D}^2 + (8\Gamma + \mathrm{i}k)\,\mathrm{D} - 2\Gamma k^2 r)\tilde{u}_z$$
$$= -k^2c^2\mathrm{i}\frac{Re}{\Gamma}\tilde{u}_r, \tag{A 9}$$

$$-\mathrm{i}k\tilde{p}_g + \left(\mathrm{D}^2 + 2\mathrm{i}\Gamma kr\,\mathrm{D} + \frac{\mathrm{D}}{r} + 4\mathrm{i}\Gamma k - 2k^2\right)\tilde{u}_z - \left(\frac{k}{r} + k\,\mathrm{D}\right)\tilde{u}_r$$
$$= -k^2c^2\frac{Re}{\Gamma}\tilde{u}_z + 2\mathrm{i}\Gamma k^2c^2\frac{Re}{\Gamma}r\tilde{u}_r, \tag{A 10}$$

where, $\mathrm{D} = \mathrm{d}/\mathrm{d}r$.

Equations (2.35)–(2.37) for the fluid and (A 8)–(A 10) for the solid must be solved with the following boundary conditions. At the tube centre, (2.41) is applicable. At $r = 1$, the linearized fluid–solid interface conditions are

$$\tilde{v}_r = -\mathrm{i}kc\tilde{u}_r, \tag{A 11}$$

$$\tilde{v}_z - 2\mathrm{i}\Gamma\tilde{u}_r = -\mathrm{i}kc\tilde{u}_z + 2\Gamma kc\tilde{u}_r, \tag{A 12}$$

$$\mathrm{D}\tilde{v}_z - k\tilde{v}_r = 4\Gamma^2 k\tilde{u}_r + \mathrm{D}\tilde{u}_z + 2\mathrm{i}\Gamma k\tilde{u}_z - k\tilde{u}_r, \tag{A 13}$$

$$-\tilde{p} + 2\mathrm{i}\,\mathrm{D}\tilde{v}_r = -\tilde{p}_g + 2\mathrm{i}\,\mathrm{D}\tilde{u}_r + 4\Gamma\,\mathrm{D}\tilde{u}_z + 4\mathrm{i}\Gamma^2\tilde{u}_r. \tag{A 14}$$

At $r = 1 + H$, boundary condition (2.67) is applicable. A comparison of the governing equations and interface conditions for the proposed Eulerian formulation obtained in § 2.2.4 and the Eulerian (CK) formulation leads to the conclusion that even though the frame of reference for both formulations is the same, the governing equations are not in agreement.

## Appendix B. Linearized fluid–solid interface conditions for L3 formulation

In this section, we derive linearized fluid–solid interface conditions for the L3 formulation given in (2.42)–(2.45). The purpose of this derivation is to demonstrate a consistent Taylor series expansion at the interface and to remove the ambiguities in the formulation of Gaurav & Shankar (2010) while deriving interface conditions in the L2 formulation. A detailed derivation of the interface conditions for the L2 formulation is provided in the work of Gaurav & Shankar (2010), and will not be discussed here.

When we use the Lagrangian frame of reference for the solid and an Eulerian frame of reference for the fluid as described in the main paper, then the material particle in the solid has the same label, irrespective of the state, because the Lagrangian frame of reference moves with the particle. Following Gaurav & Shankar (2010), we will denote the position of the interface particle as $P$, fluid and solid dynamical quantities with $F$ and $S$, respectively. Consider a particle at the interface at time $t = 0$ at $P_0(R = 1, Z)$. Because of the fluid motion, the solid will deform, which we call here the pre-stressed state and the position of the particle will be, $P(\bar{r} = 1, \bar{z})$. On this pre-stressed state, we impose small perturbations after which the particle will move to $P'(r = (\bar{r} = 1) + u'_r, z = \bar{z} + u'_z)$. Hence, schematically, the interface conditions for the L3 formulation at the interface could be written as,

$$F(r, z, t)|_{P'} = S(\bar{r}, \bar{z}, t)|_{P'}. \tag{B 1}$$

To clarify the procedure, we will use following relations,

$$F(r, z, t)|_{P'} = \bar{F}(r, z)|_{P'} + F'(r, z, t)|_{P'}, \tag{B 2}$$

$$S(\bar{r}, \bar{z}, t)|_{P'} = \bar{S}(\bar{r}, \bar{z})|_{P'} + S'(\bar{r}, \bar{z}, t)|_{P'}, \tag{B 3}$$

where the first term in each of the above equations denotes a base state quantity while the second term denotes a perturbed state quantity.

Before proceeding with the derivation of the boundary condition it is relevant to reiterate the purpose of Taylor expansion. For L3 formulation, while deriving base state, tangential and normal stress balances are taken at the pre-stressed interface. For a representative interface particle, that position, as discussed above, is $P(\bar{r} = 1, \bar{z})$. Hence, in base state, the interface conditions schematically can be represented as,

$$\bar{F}(\bar{r}, \bar{z})|_P = \bar{S}(\bar{r}, \bar{z})|_P. \tag{B 4}$$

After imposing perturbations, the velocity and stress balances are to be taken at the perturbed interface for which the position of the particle is $P'(r = \bar{r} + u'_r, z = \bar{z} + u'_z)$. Hence (B 1) becomes

$$\bar{F}(r, z)|_{P'} + F'(r, z, t)|_{P'} = \bar{S}(\bar{r}, \bar{z})|_{P'} + S'(\bar{r}, \bar{z}, t)|_{P'}. \tag{B 5}$$

As noted above, the base state stress balances are carried out about the pre-stressed state interface which implies that, to equate the base state terms on the fluid and solid sides, both must be brought back to the pre-stressed state interface. To achieve this, we note that the solid quantities are already functions of the pre-stressed variables, but for the fluid quantities we need Taylor series expansion. This can be schematically represented as,

$$\bar{S}(\bar{r}, \bar{z})|_{P'} = \bar{S}(\bar{r}, \bar{z})|_P, \tag{B 6}$$

$$F(r, z)|_{P'} = \bar{F}(\bar{r}, \bar{z})|_P + u'_r(\bar{r} = 1, \bar{z}, t)\left(\frac{\partial \bar{F}(\bar{r}, \bar{z})}{\partial \bar{r}}\right)_P + u'_z(\bar{r} = 1, \bar{z}, t)\left(\frac{\partial \bar{F}(\bar{r}, \bar{z})}{\partial \bar{z}}\right)_P. \tag{B 7}$$

Substituting the above equations in (B 5) and cancelling the base state term we arrive at the final boundary condition,

$$\begin{aligned} &u'_r(\bar{r} = 1, \bar{z}, t)\left(\frac{\partial \bar{F}(\bar{r}, \bar{z})}{\partial \bar{r}}\right)_P + u'_z(\bar{r} = 1, \bar{z}, t)\left(\frac{\partial \bar{F}(\bar{r}, \bar{z})}{\partial \bar{z}}\right)_P + F'(r, z, t)|_{P'} \\ &\quad = S'(\bar{r}, \bar{z}, t)|_{P'}. \end{aligned} \tag{B 8}$$

To demonstrate the use of above discussion, we consider the linearized tangential velocity continuity and normal stress continuity at the interface. Using above discussion, the continuity of tangential velocity at the perturbed fluid–solid interface is given by

$$v_z(r, z, t)|_{P'} = \left(\frac{\partial z}{\partial t}\right)_{P'}. \tag{B 9}$$

But, in this case $\bar{F}(\bar{r}, \bar{z}) = \bar{v}_z(\bar{r}, \bar{z}) = \Gamma(1 - r^2)$, hence in linearized form the above equation becomes,

$$v'_z(r = 1, z, t) - 2\Gamma u'_r(\bar{r} = 1, \bar{z}, t) = \left(\frac{\partial u'_z}{\partial t}\right)_{\bar{r}=1, \bar{z}=z}. \tag{B 10}$$

Now using normal modes in above equation we obtain,

$$\tilde{v}_z(r = 1) - 2\Gamma \tilde{u}_r(\bar{r} = 1) = -\mathrm{i}kc\tilde{u}_z(\bar{r} = 1). \tag{B 11}$$

Comparing the above equation with the tangential velocity continuity equation given in Gaurav & Shankar (2010) shows that there will not be any extra exponential term multiplying the fluid side, unlike the case of the L2 formulation of Gaurav & Shankar (2010). This also means that there will not be any need for subsequent modification to the fluid side governing equations, which was necessary in the case of L2 formulation.

For deriving the linearized normal stress balance, substituting $\bar{F}(\bar{r},\,\bar{z}) = -\bar{p}(\bar{z})$ in (B 8) along with normal stress components and simplifying we obtain,

$$\begin{aligned} &-p'(r=1) + 2\partial_r v_r'(r=1) - \frac{\mathrm{d}\bar{p}_g}{\mathrm{d}z} u_z'(\bar{r}=1) \\ &\quad = -p_g'(\bar{r}=1) + 2(1+\eta_r\partial_t)\partial_r u_r'(\bar{r}=1) - 4\Gamma\partial_z u_r'(\bar{r}=1). \end{aligned} \tag{B 12}$$

Substituting $\mathrm{d}\bar{p}_g/\mathrm{d}z = -4\Gamma$ and using the normal modes in above equation we obtain the final form as

$$\begin{aligned} &-\tilde{p}(r=1) + 2\mathrm{i}\,\mathrm{D}\tilde{v}_r(r=1) \\ &\quad = -\tilde{p}_g(\bar{r}=1) + 2\mathrm{i}(1-\mathrm{i}kc\eta_r)\,\mathrm{D}\tilde{u}_r(\bar{r}=1) + 4\Gamma k\tilde{u}_r(\bar{r}=1) - 4\Gamma\tilde{u}_z(\bar{r}=1). \end{aligned} \tag{B 13}$$

The last term on the right-hand side of the above equation plays a major role in determining the stability behaviour which will be elaborated in the sequel to the present work. Following the same procedure, the other two linearized interface conditions (2.43)–(2.44) can be derived.

## Appendix C. Linearized perturbation equations for plane Couette flow in the L3 formulation

In this appendix, we briefly outline the base state and linearized equations for plane Couette flow in the modified L3 formulation. The velocity of fluid and deformation in solid in base state are

$$\bar{v}_x = \Gamma y; \quad \bar{u}_x = \Gamma(\bar{y}+H), \tag{C 1a,b}$$

where $\Gamma = V\eta/(GL)$ and $L$ is the thickness of the fluid layer.

The linearized perturbation equations for the fluid, with $\mathrm{D} = \mathrm{d}/\mathrm{d}y$, are

$$\mathrm{D}\tilde{v}_y + \mathrm{i}k\tilde{v}_x = 0, \tag{C 2}$$

$$-\mathrm{i}k\tilde{p}_g + (\mathrm{D}^2 - k^2)\tilde{v}_x = \frac{Re}{\Gamma}[\mathrm{i}k(\bar{v}_x - c) + \mathrm{D}\bar{v}_x]\tilde{v}_x, \tag{C 3}$$

$$-\mathrm{D}\tilde{p} + (\mathrm{D}^2 - k^2)\tilde{v}_y = \frac{Re}{\Gamma}[\mathrm{i}k(\bar{v}_x - c)]\tilde{v}_y. \tag{C 4}$$

Similarly, the linearized perturbation equations for the solid are

$$\mathrm{D}\tilde{u}_y + \mathrm{i}k\tilde{u}_x = 0, \tag{C 5}$$

$$\begin{aligned} &-\mathrm{i}k\tilde{p}_g + (1-\mathrm{i}kc\eta_r)(\mathrm{D}^2 - k^2)\tilde{u}_x - \Gamma^2k^2\tilde{u}_x + 2\mathrm{i}k\Gamma\,\mathrm{D}\tilde{u}_x \\ &\qquad = -\frac{Re}{\Gamma}k^2c^2\tilde{u}_x, \end{aligned} \tag{C 6}$$

$$\begin{aligned} &-\mathrm{D}\tilde{p}_g + (1-\mathrm{i}kc\eta_r)(\mathrm{D}^2 - k^2)\tilde{u}_y - \Gamma^2k^2\tilde{u}_y + 2\mathrm{i}k\Gamma\,\mathrm{D}\tilde{u}_y \\ &\qquad = -\frac{Re}{\Gamma}k^2c^2\tilde{u}_y. \end{aligned} \tag{C 7}$$

At $y=1$, the boundary conditions are

$$\tilde{v}_x = 0; \quad \tilde{v}_y = 0. \tag{C 8a,b}$$

At the fluid–solid interface ($y=0$), the linearized continuity conditions are

$$\tilde{v}_x + \Gamma\tilde{u}_y + \mathrm{i}kc\tilde{u}_x = 0, \tag{C 9}$$

$$\tilde{v}_z + \mathrm{i}kc\tilde{u}_y = 0, \tag{C 10}$$

$$(1 - \mathrm{i}kc\eta_r)(\mathrm{i}k\tilde{u}_y + \mathrm{D}\tilde{u}_x) - \mathrm{D}\tilde{v}_x - \mathrm{i}k\tilde{v}_y = 0, \tag{C 11}$$

$$\tilde{p}_g - 2(1 - \mathrm{i}kc\eta_r)\,\mathrm{D}\tilde{u}_y - 2\mathrm{i}k\Gamma\tilde{u}_y - \tilde{p}_f + 2\,\mathrm{D}\tilde{v}_y = 0. \tag{C 12}$$

At $y=-H$ the boundary conditions are

$$\tilde{u}_x = 0; \quad \tilde{u}_y = 0. \tag{C 13a,b}$$

## REFERENCES


BENJAMIN, T. B. 1960 Effect of a flexible surface on boundary layer stability. *J. Fluid Mech.* **9**, 513–532.

BENJAMIN, T. B. 1963 The threefold classification for unstable disturbances in flexible surfaces bounding inviscid flows. *J. Fluid Mech.* **16**, 436–450.

BIRD, R. B., ARMSTRONG, R. C. & HASSAGER, O. 1977 *Dynamics of Polymeric Liquids,* Vol. 1 *Fluid Mechanics*. John Wiley.

BOYD, J. P. 2001 *Chebyshev and Fourier Spectral Methods*, 2nd edn. Dover.

CARPENTER, P. W. & MORRIS, P. J. 1990 The effect of anisotropic wall compliance on boundary-layer stability and transition. *J. Fluid Mech.* **218**, 171–223.

CARPENTER, P. W. & GAJJAR, J. S. B. 1990 A general theory for two and three dimensional wall-mode instabilities in boundary layers over isotropic and anisotropic compliant walls. *Theor. Comput. Fluid Dyn.* **1**, 349–378.

CARPENTER, P. W. & GARRAD, A. D. 1985 The hydrodynamic stability of flows over Kramer-type compliant surfaces. Part 1. Tollmien–Schlichting instabilities. *J. Fluid Mech.* **155**, 465–510.

CARPENTER, P. W. & GARRAD, A. D. 1986 The hydrodynamic stability of flows over Kramer-type compliant surfaces. Part 2. flow induced surface instabilities. *J. Fluid Mech.* **170**, 199–232.

CHOKSHI, P. & KUMARAN, V. 2007 Stability of the flow of a viscoelastic fluid past a deformable surface in the low Reynolds number limit. *Phys. Fluids* **19**, 104103.

CHOKSHI, P. & KUMARAN, V. 2008*a* Weakly nonlinear analysis of viscous instability in flow past a neo-Hookean surface. *Phys. Rev.* E **77**, 056303.

CHOKSHI, P. & KUMARAN, V. 2008*b* Weakly nonlinear stability analysis of a flow past a neo-Hookean solid at arbitrary Reynolds numbers. *Phys. Fluids* **20**, 094109.

DAVIES, C. & CARPENTER, P. W. 1997 Instabilities in a plane channel flow between compliant walls. *J. Fluid Mech.* **352**, 205–243.

DESTARDE, M. & SACCOMANDI, G. 2004 Finite–amplitude inhomogeneous waves in Mooney–Rivlin viscoelastic solids. *Wave Motion* **40**, 251–262.

DRAZIN, P. G. & REID, W. H. 1981 *Hydrodynamic Stability*. Cambridge University Press.

EGGERT, M. D. & KUMAR, S. 2004 Observations of instability, hysterisis, and oscillation in low-Reynolds number flow past polymer gels. *J. Colloid Interface Sci.* **278**, 234–242.

GARG, V. K. 1977 Effect of tube elasticity on the stability of Poiseuille flow. *J. Fluid Mech.* **81**, 625–640.

GAURAV & SHANKAR, V. 2009 Stability of fluid flow through deformable neo-Hookean tubes. *J. Fluid Mech.* **627**, 291–322.

GAURAV & SHANKAR, V. 2010 Stability of pressure-driven flow in a deformable neo-Hookean channel. *J. Fluid Mech.* **659**, 318–350.

GIRIBABU, D. & SHANKAR, V. 2016 Consistent formulation of solid dissipative effects in stability analysis of flow past a deformable solid. *Phys. Rev. Fluids* **1**, 033602.

GKANIS, V. & KUMAR, S. 2003 Instability of creeping Couette flow past a neo-Hookean solid. *Phys. Fluids* **15**, 2864–2871.

GKANIS, V. & KUMAR, S. 2005 Stabilty of pressure-driven creeping flows in channels lined with a nonlinear elastic solid. *J. Fluid Mech.* **524**, 357–375.

GROTBERG, J. B. 2011 Respiratory fluid mechanics. *Phys. Fluids* **23** (2), 021301.

GROTBERG, J. B. & JENSEN, O. E. 2004 Biofluid mechanics in flexible tubes. *Annu. Rev. Fluid Mech.* **36**, 121–147.

HOLZAPFEL, G. A. 2000 *Nonlinear Solid Mechanics*. John Wiley.

KRINDEL, P. & SILBERBERG, A. 1979 Flow through gel-walled tubes. *J. Colloid Interface Sci.* **71**, 34–50.

KUMARAN, V. 1995*a* Stability of the flow of a fluid through a flexible tube at high Reynolds number. *J. Fluid Mech.* **302**, 117–139.

KUMARAN, V. 1995*b* Stability of the viscous flow of a fluid through a flexible tube. *J. Fluid Mech.* **294**, 259–281.

KUMARAN, V. 1998 Stability of fluid flow through a flexible tube at intermediate Reynolds number. *J. Fluid Mech.* **357**, 123–140.

KUMARAN, V. 2003 Hydrodynamic stability of flow through compliant channels and tubes. In *IUTAM symposium on flow past highly compliant boundaries and in collapsible tubes* (ed. P. W. Carpenter & T. J. Pedley), chap. 5, pp. 95–118. Kluwer.

KUMARAN, V. 2015 Experimental studies on the flow through soft tubes and channels. *Sadhana* **40**, 911–923.

KUMARAN, V. & BANDARU, P. 2016 Ultra-fast microfluidic mixing by soft-wall turbulence. *Chem. Engng Sci.* **149**, 156–168.

KUMARAN, V., FREDRICKSON, G. H. & PINCUS, P. 1994 Flow induced instability of the interface between a fluid and a gel at low Reynolds number. *J. Phys. II France* **4**, 893–904.

KUMARAN, V. & MURALIKRISHNAN, R. 2000 Spontaneous growth of fluctuations in the viscous flow of a fluid past a soft interface. *Phys. Rev. Lett.* **84**, 3310–3313.

LANDAHL, M. T. 1962 On the stability of a laminar incompressible boundary layer over a flexible surface. *J. Fluid Mech.* **13**, 609.

LARSON, R. G. 1988 *Constitutive Equations for Polymer Melts and Solutions*. Butterworths.

LARSON, R. G. 1999 *The Structure and Rheology of Complex Fluids*. Oxford University Press.

LEE, S. H., MAKI, K. L., FLATH, D., WEINSTEIN, S. J., KEALEY, C., LI, W., TALBOT, C. & KUMAR, S. 2014 Gravity-driven instability of a thin liquid film underneath a soft solid. *Phys. Rev.* E **90**, 053009.

MA, Y. & NG, C.-O. 2009 Wave propagation and induced steady streaming in viscous fluid contained in a prestressed viscoelastic tube. *Phys. Fluids* **21**, 051901.

MACOSKO, C. W. 1994 *Rheology: Principles, Measurements, and Applications*. VCH.

MALVERN, L. E. 1969 *Introduction to the Mechanics of a Continuous Medium*. Prentice-Hall.

MCDONALD, J. C. & WHITESIDES, G. M. 2002 Poly(dimethylsiloxane) as a material for fabricating microfluidic devices. *Acc. Chem. Res.* **35**, 491–499.

NEELAMEGAM, R. & SHANKAR, V. 2015 Experimental study of the instability of laminar flow in a tube with deformable walls. *Phys. Fluids* **27**, 024102.

NORRIS, A. N. 2007 Small-on-large theory with applications to granular materials and fluid/solid systems. In *Waves in Nonlinear Pre-Stressed Materials* (ed. M. Destrade & G. Saccomandi), pp. 27–62. Springer.

NORRIS, A. N. 2008 Eulerian conjugate stress and strain. *J. Mech. Mater. Struct.* **3**, 243–260.

SCHMID, P. J. & HENNINGSON, D. S. 2001 *Stability and Transition in Shear Flows*. Springer.

SHANKAR, V. 2015 Stability of fluid flow through deformable tubes and channels: an overview. *Sadhana* **40**, 925–943.

SHANKAR, V. & KUMARAN, V. 1999 Stability of non-parabolic flow in a flexible tube. *J. Fluid Mech.* **395**, 211–236.

SHANKAR, V. & KUMARAN, V. 2000 Stability of fluid flow in a flexible tube to non-axisymmetric disturbances. *J. Fluid Mech.* **408**, 291–314.

SHANKAR, V. & KUMARAN, V. 2001 Weakly nonlinear stability of viscous flow past a flexible surface. *J. Fluid Mech.* **434**, 337–354.

SHANKAR, V. & KUMARAN, V. 2002 Stability of wall modes in fluid flow past a flexible surface. *Phys. Fluids* **14**, 2324–2338.

SHRIVASTAVA, A., CUSSLER, E. L. & KUMAR, S. 2008 Mass transfer enhancement due to a soft elastic boundary. *Chem. Engng Sci.* **63**, 4302–4305.

SQUIRES, T. M. & QUAKE, S. R. 2005 Microfluidics: fluid physics at the nanoliter scale. *Rev. Mod. Phys.* **77**, 977–1026.

SRINIVAS, S. S. & KUMARAN, V. 2015 After transition in a soft-walled microchannel. *J. Fluid Mech.* **780**, 649–686.

SRINIVAS, S. S. & KUMARAN, V. 2017 Effect of viscoelasticity on the soft-wall transition and turbulence in a microchannel. *J. Fluid Mech.* **812**, 1076–1118.

TOUPIN, R. A. & BERNSTEIN, B. 1961 Sound waves in deformed perfectly elastic materials: acoustoelastic effect. *J. Acoust. Soc. Am.* **33**, 216–225.

VERMA, M. K. S. & KUMARAN, V. 2012 A dynamical instability due to fluid-wall coupling lowers the transition Reynolds number in the flow through a flexible tube. *J. Fluid Mech.* **705**, 322–347.

VERMA, M. K. S. & KUMARAN, V. 2013 A multifold reduction in the transition Reynolds number, and ultra-fast mixing, in a micro-channel due to a dynamical instability induced by a soft wall. *J. Fluid Mech.* **727**, 407–455.

VERMA, M. K. S. & KUMARAN, V. 2015 Stability of flow in a soft tube deformed due to applied pressure gradient. *Phys. Rev.* E **91**, 043001.